Supplemental Figures.

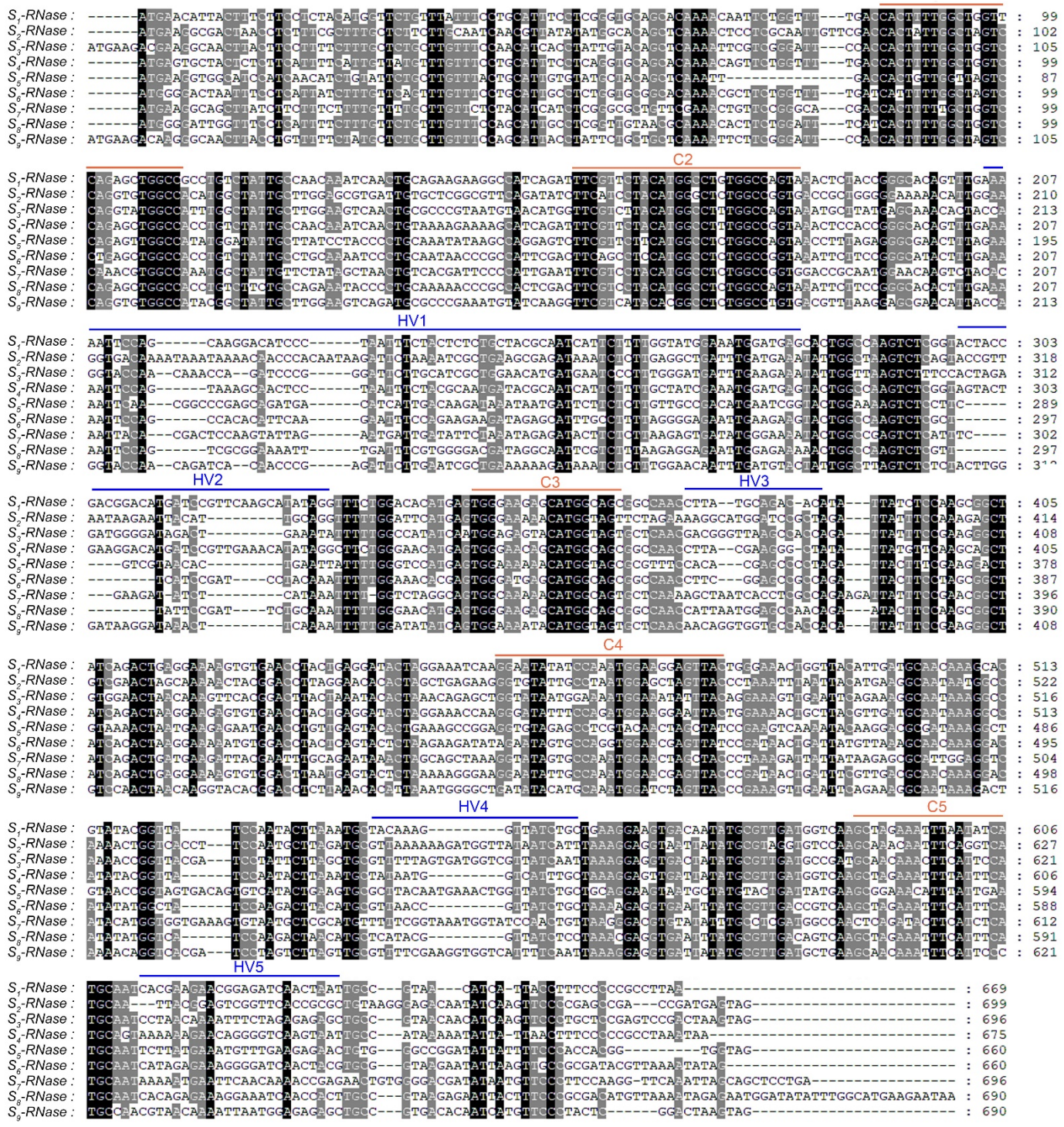

Supplementary Figure 1. Nucleotide sequence alignments for the pummelo *S*$_1$-RNase – *S*$_9$-RNases.

The nucleotide sequence identities above 80% among *S-RNase*s are indicated by shaded boxes: *black indicates* 100% conservation; *grey* indicates ≥ 80% conservation; *dashes* represent gaps. The citrus *S-RNase*s contain five conserved domains (C1-C5) and five hypervariable regions (HV1-HV5).

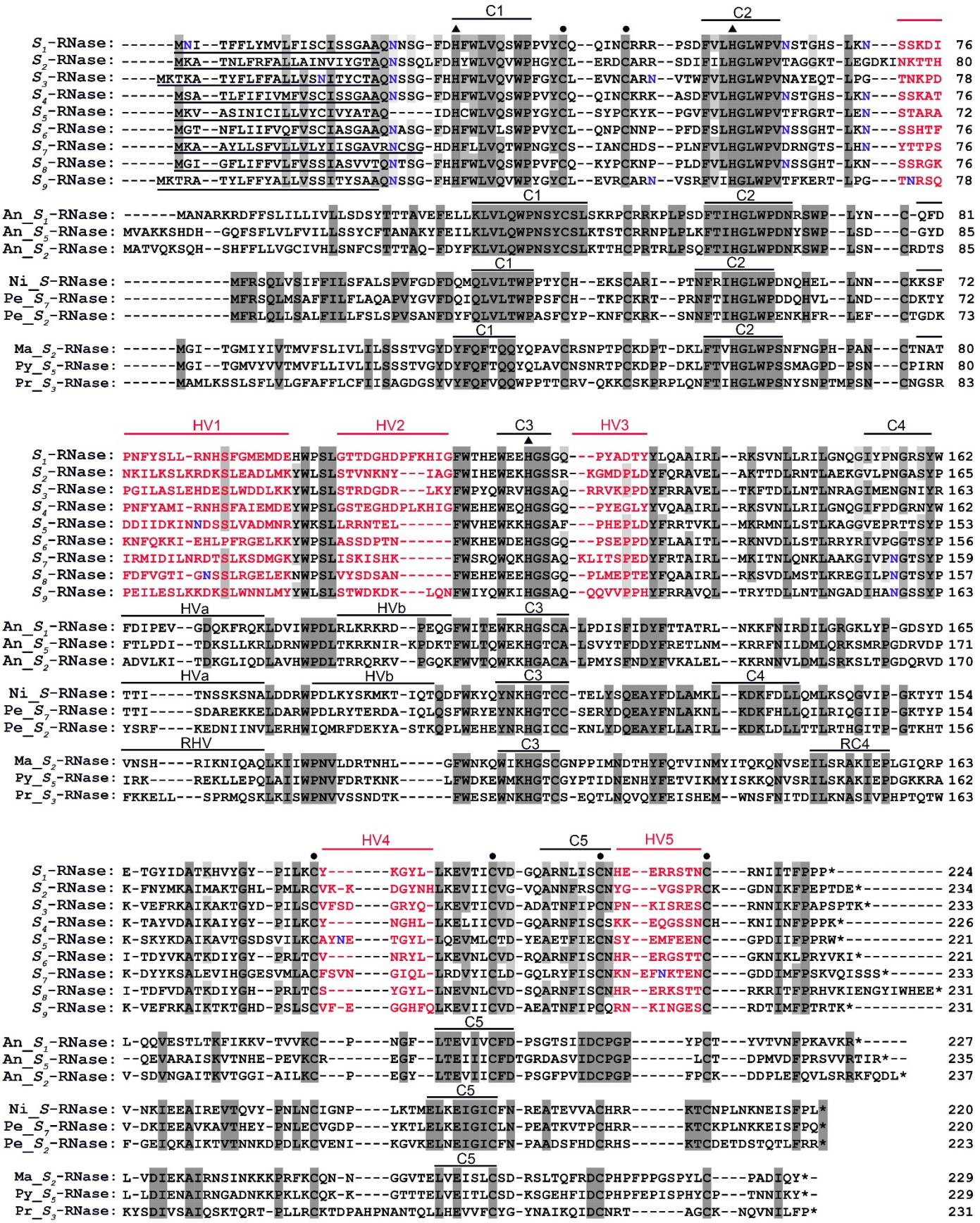

Supplementary Figure 2. Amino acid sequence alignments of *S*-RNases from pummelo and Plantaginaceae (prefix An for *Antirrhinum*) and Solanaceae (prefixes Ni and Pe for *Nicotiana* and *Petunia*) and Rosaceae (prefixes Ma, Py and Pr for *Malus*, *Pyrus* and *Prunus*).

The pummelo *S*-RNase sequences used are S_1-RNase to S_9-RNase; Plantaginaceae *S*-RNase sequences (An_S1-RNase: HE805271, An_S5-RNase: X96464, An_S2-RNase: X96465), Solanaceae *S*-RNase

sequences (Ni_S-RNase: CAA05306, Pe_S7-RNase: BAJ24847 and Pe_S2-RNase: AAG21384) and Rosaceae *S*-RNase sequences (Ma_S2-RNase: ADB85476, Py_S5-RNase: BAA13577 and Pr_S3-RNase: CAC27786) were downloaded from the NCBI protein database.

The conserved amino acids of *S*-RNases from pummelo, Plantaginaceae, Solanaseae and Rosaceae, respectively, are indicated by shaded boxes (grey indicates 100% identity; light grey ≥ 70% identity). The *S*-RNases from pummelo contain five conserved domains (C1-C5) and five hypervariable regions (HV1- HV5, indicated in red). HV1 and HV2 have the highest diversity and correspond to HVa and HVb of the *S*-RNases from Plantaginaceae and Solanaceae.

The three conserved histidine residues (triangles), six conserved cysteine residues (solid circles), and an amino-terminal signal peptide (underlined) present in the pummelo sequences are indicated. The asparagine amino acid residues (N), predicted to be potentially N-glycosylated, are indicated in blue font. The S_2-RNase has 1 such potentially N-glycosylated amino acids; S_3-, S_4-, S_5- and S_6-RNase have 3; S_1-, S_7-, S_8- and S_9-RNase have 4 potentially N-glycosylated asparagine amino acids.

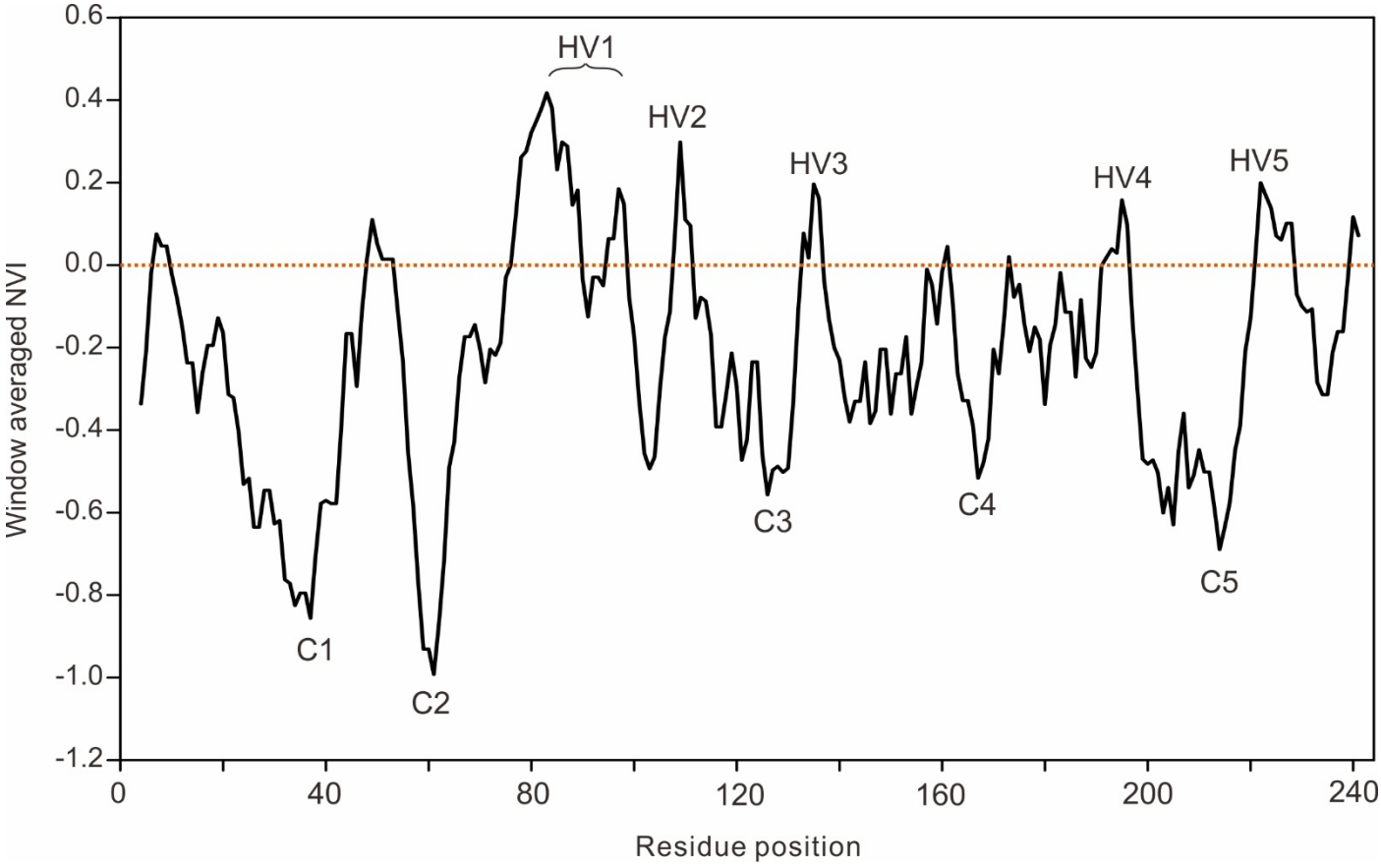

Supplementary Figure 3. Normed Variability Index (NVI) figure calculating the conserved and hypervariable sequences present in the nine pummelo *S*-RNases.

The averaged NVI value of each residue is calculated using a window of seven residues as described by Kheyr-Pour et al[1]. Analysis of the nine pummelo putative *S*-RNase sequences revealed five conserved regions (the valleys, C1- C5) and five hypervariable regions (the peaks, HV1- HV5). HV1 and HV2 have the highest sequence diversity so are the most polymorphic between the citrus sequences.

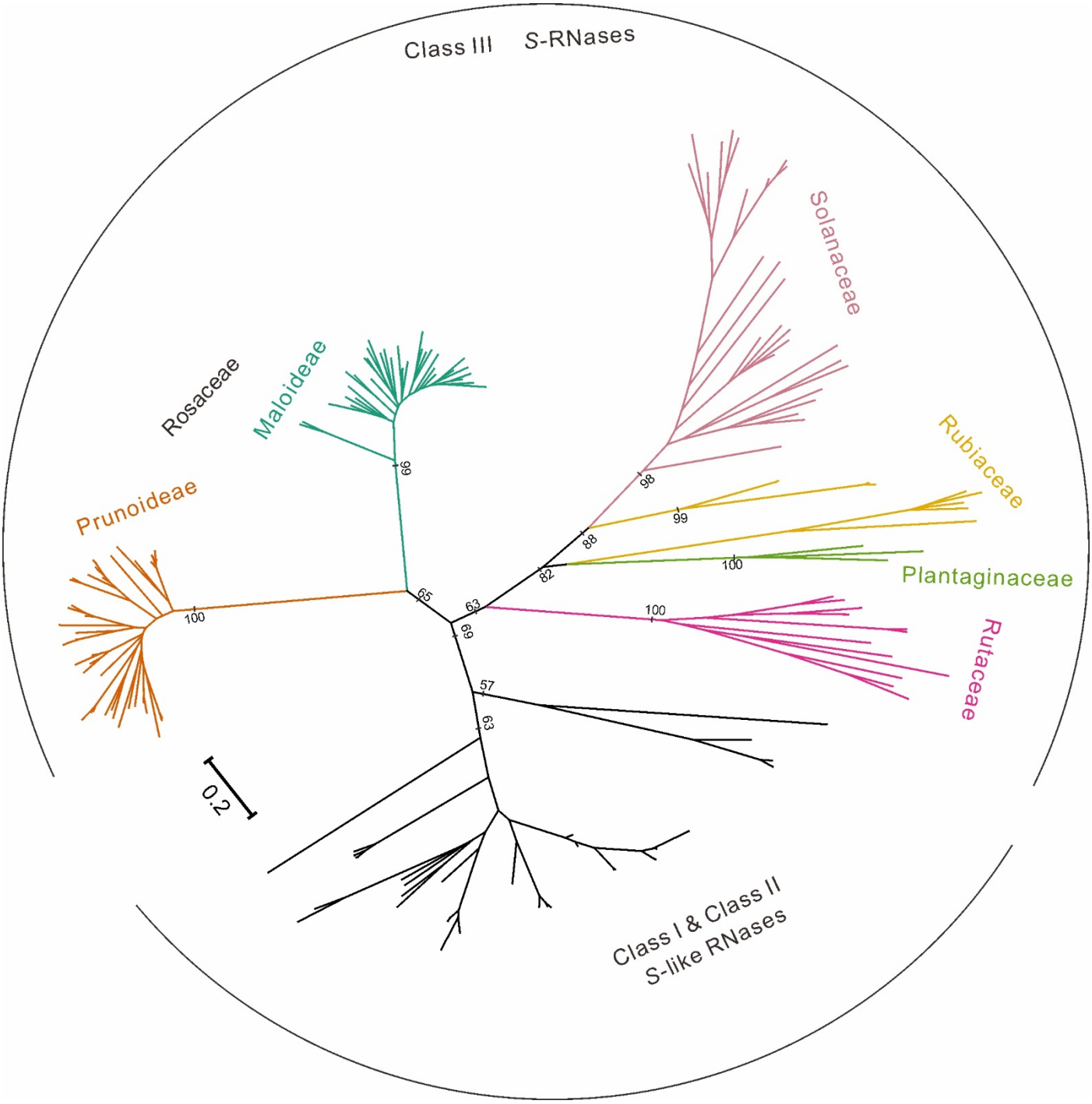

Supplementary Figure 4. Phylogeny of the *S*-RNases identified in pummelo (Rutaceae) and known *S*-RNases from Rosaceae, Solanaceae, Plantaginaceae and Rubiaceae.

The phylogenetic tree was constructed with deduced amino acid sequences using the maximum likelihood method with 1000 rapid bootstraps. The *S*-like RNase sequence from *Bryopsis maxima* (AB164318) was used as an outgroup. Genome-wide identification of T2/*S*-type ribonucleases in 'Wanbai' pummelo was carried out with HMMER[2] based on Liang's method[3] and the identified *S*-RNases were also submitted to the phylogenetic analysis. The putative Rubiaceae (*Coffea*) sequences[4,5] are also indicated here for completeness and for comparison.

The T2/*S*-type ribonucleases grouped into Class I, II and III, as reported by Ramanauskas and Igić[6]. All functional *S*-RNases fall into the Class III clade). The class III T2/*S*-type RNases from the Roseaceae (Prunoideae and Maloideae) are well separated from the other class III T2/*S*-type RNases from the Solanaceae, Plantaginaceae and putative *S*-type RNases from the Rubiaceae. The *S*-type RNases from pummelo (Rutaceae) clustered together on an independent branch.

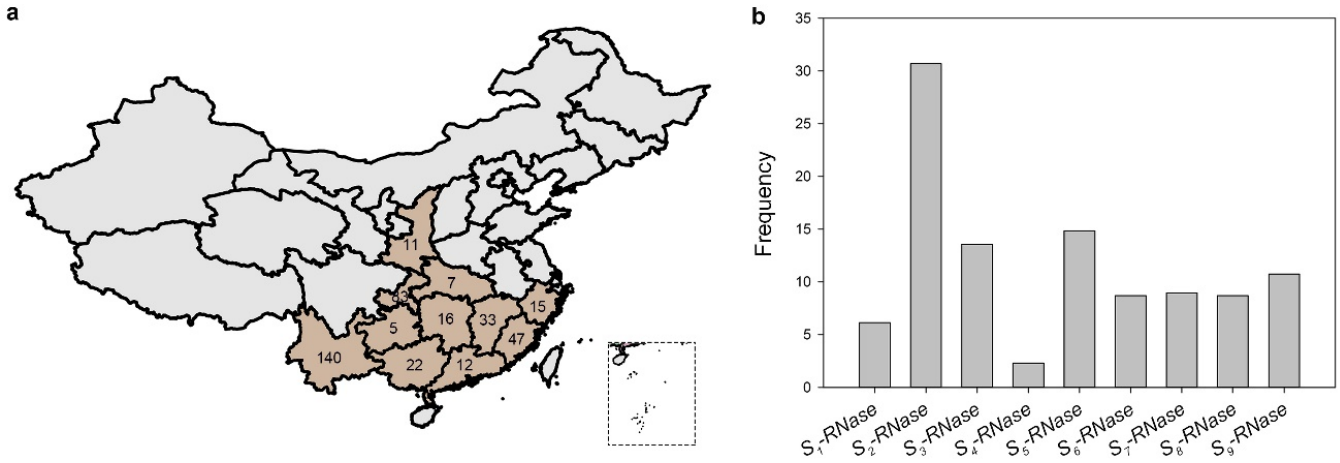

Supplementary Figure 5. Analysis of the *S*-haplotype of 391 Chinese pummelo accessions.

(a) The distribution of 391 Chinese pummelo accessions. 391 pummelo accessions were collected from 11 provinces (brown) in China. The number of accessions from each province is indicated on the map.

(b) The frequency of *S_1-RNase* to *S_9-RNase* in 391 pummelo accessions. The nine *S-RNase*s identified, *S_1-RNase* to *S_9-RNase* were found in 76.2% of these accessions. Most occur at a low frequency, as expected for negative frequency dependent selection. The *S_2-RNase* is present at the highest frequency with 30.2%. *S_4-RNase* is present at the lowest frequency with 2.3%.

The *S*-haplotype of these pummelo accessions were assigned using PCR of leaf DNA with *S-RNase* (*S_1-RNase* to *S_9-RNase*) specific primers.

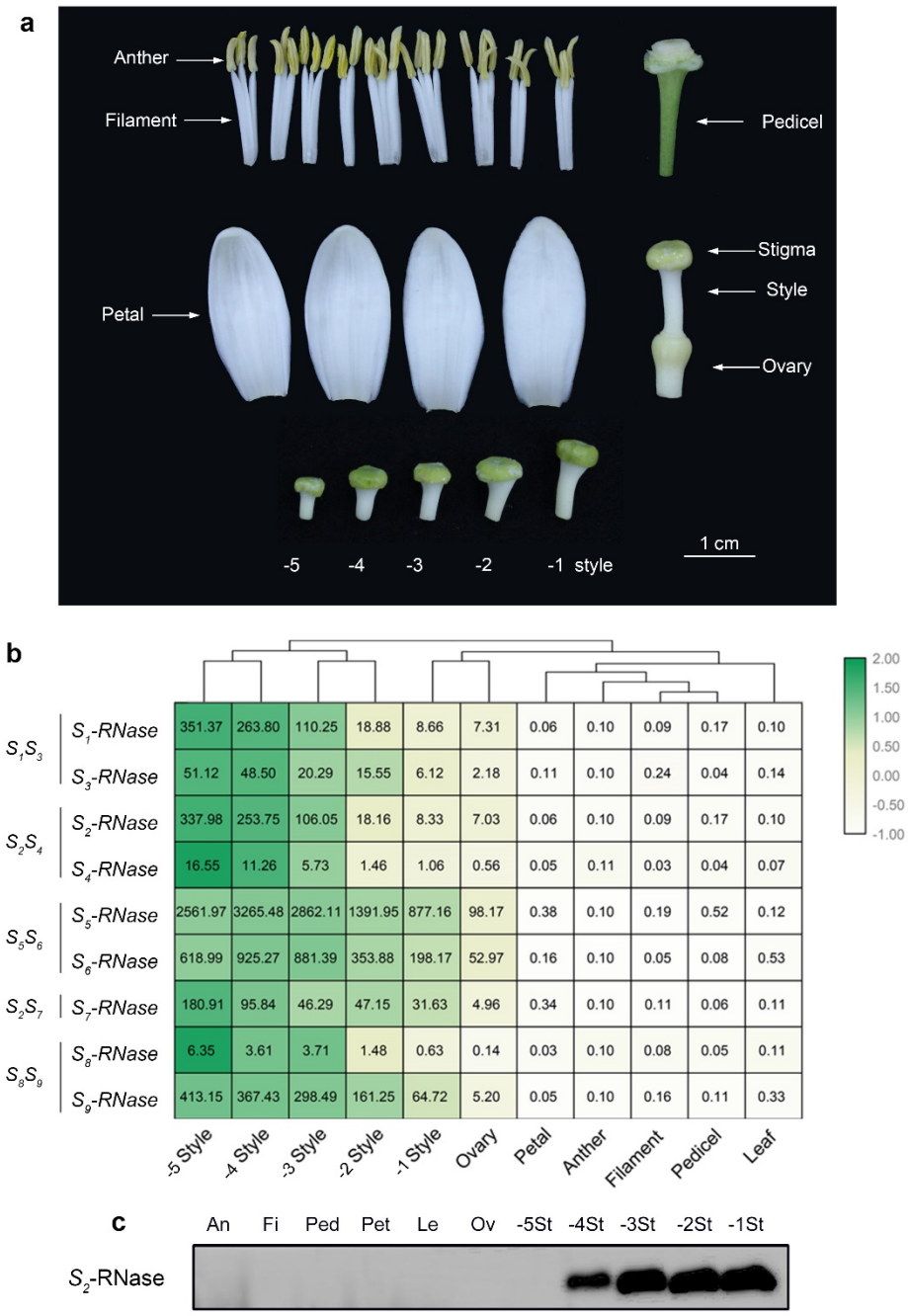

Supplementary Figure 6. Morphology of pummelo floral organs and pistils at different developmental stages and expression of the *S*-RNases.

(a) Images of pummelo floral organs. Top row: anthers, filaments and pedicel (stage 0 = open flower); middle row: petal and pistil (stage 0 = open flower); bottom row: pistils (stigma and style) at five stages during development: -5, -4, -3, -2, and -1 indicate days relative to anthesis; the mature style is ~1 cm in length.

(b) qPCR showing temporal and tissue-specific expression of *S*$_1$- to *S*$_9$-*RNase* transcripts. The heat map shows the relative expression of nine *S-RNase* genes quantified using qRT-PCR in styles at different developmental stages: -5, -4, -3, -2, and -1 days before anthesis. An: anther; Fi: filament; Ped: pedicel; Pet: petal; Le: leaf; Ov: ovary; St: style. The scale bar (right) indicates expression levels (log_2-transformed values). The mean transcript level (based on three biological replicates), is shown in each box.

(c) Western blot showing expression of the *S*$_2$-RNase protein in various tissues and in pistils at different developmental stages (*S*$_1$*S*$_2$ genotype). There was no expression in tissues except in style (St). In contrast to the transcript (see b), which peaked at -5 days and subsequently declined, protein levels were not detected at this early stage, and increased over time as the pistil matured. Experiments were repeated independently twice three times with similar results obtained for each.

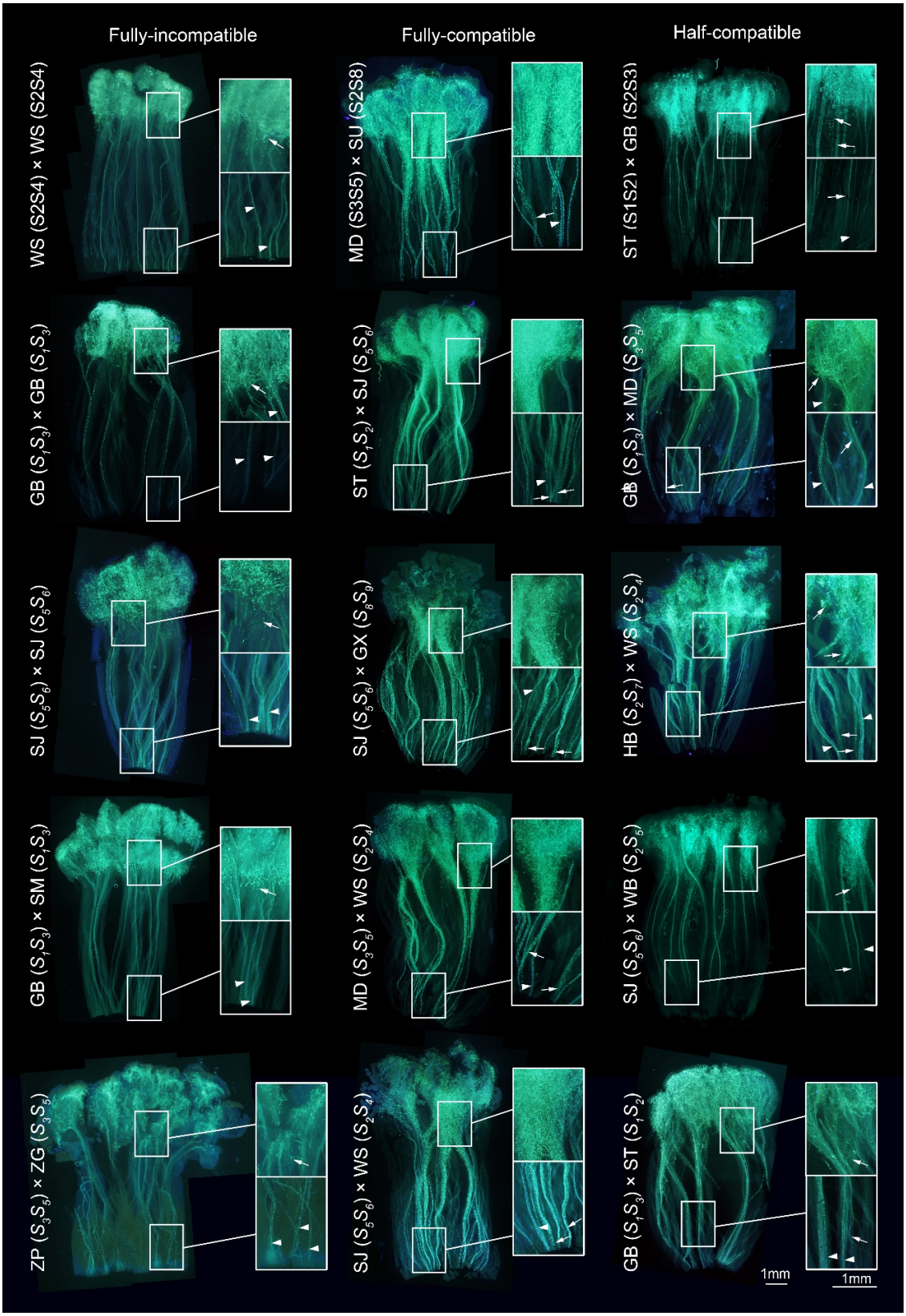

Supplementary Figure 7. Representative pollinated pummelo pistils stained with aniline blue. Representative images (5 of each type of pollination, 15 in total) of aniline blue staining of pollinated pummelo pistils (5 days after pollination) classified in Supplementary Table 3. The accession names and their respective *S*-genotypes are indicated to the left of each block.
In fully-incompatible crosses, pollen tubes were inhibited near the top of the style (upper inset panel) and no significant long pollen tubes were observed in the style (lower inset panel); In fully-compatible crosses, bunches of pollen tubes extended through the pistil. In the half-compatible crosses; some pollen tubes extended to the base of the pistil, while others were inhibited near the top of the style. Pollen tubes (pt) are indicated with arrows. Vascular bundles (vb) are indicated with arrowheads. At least two pistils of each pollination combinations were observed (see **Supplementary Table 5**).

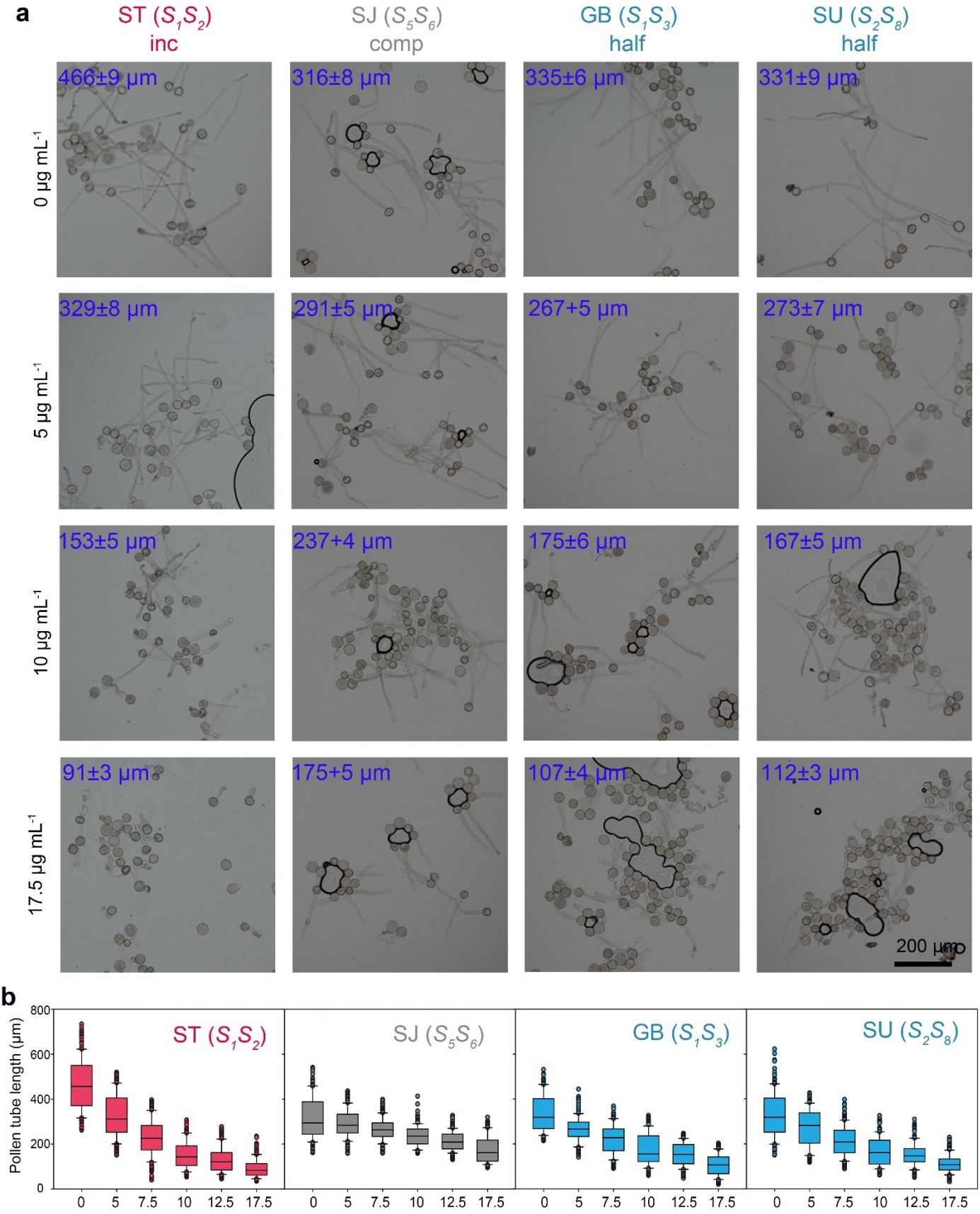

Supplementary Figure 8. Effect of a dilution series of recombinant pummelo S_1- and S_2-RNases on pollen tubes growing *in vitro*, showing increasing inhibitory activity (and some non-specific inhibitory activity).

(a) Representative images of the effect of a dilution series of *S*-RNase treatments on pummelo pollen tube growth using the *in vitro* bioassay. The concentrations of combined S_1-RNase and S_2-RNase are indicated at the left hand side of the panel (e.g. 5 µg mL^{-1} indicates 5 µg mL^{-1} S_1-RNase + 5 µg mL^{-1} S_2-

RNase as a combined treatment). The mean pollen tube length ± SEM for each treatment is shown in the upper left hand side of the corresponding representative image; > fifty pollen tubes were measured in three independent experiments (> 150 in total).

(b) Box plot showing quantitation of pollen tube length measured for the ST (*S_1S_2*), SJ (*S_5S_6*), GB (*S_1S_3*) and SU (*S_2S_8*) pummelo accessions. When treated with 10 μg mL^{-1} *S_1*-RNase and 10 μg mL^{-1} *S_2*-RNase combined, pollen from plants with genotype *S_1S_2* (an incompatible combination, red) showed a ~67% decrease in length compared to the untreated controls. *S_5S_6* pollen (a compatible combination, grey) showed some non-specific activity at higher concentrations. Pollen from plants of genotype *S_1S_3* or *S_2S_8* pollen (a half-compatible combination, blue) showed an overall ~50% decrease in pollen tube length. These dilution series were used to ascertain the optimal concentrations of *S_1*- and *S_2*-RNases for the in vitro SI bioassay. On the basis of these tests, a concentration of 10 μg mL^{-1} was chosen for all the key test assays in this study, to obtain maximal inhibition with minimal non-specific activity. The length of >50 pollen tubes was measured for each replicate (n = 3 biologically independent replicates, >150 in total). Box and whisker plots show the distribution of individual pollen tube lengths in *in vitro* bioassays of recombinant S_1- and S_2-RNases with pollen from plants of different genotypes (box indicates the upper & lower quartile, with median; lines above and below indicate the range; dots indicate the outliers).

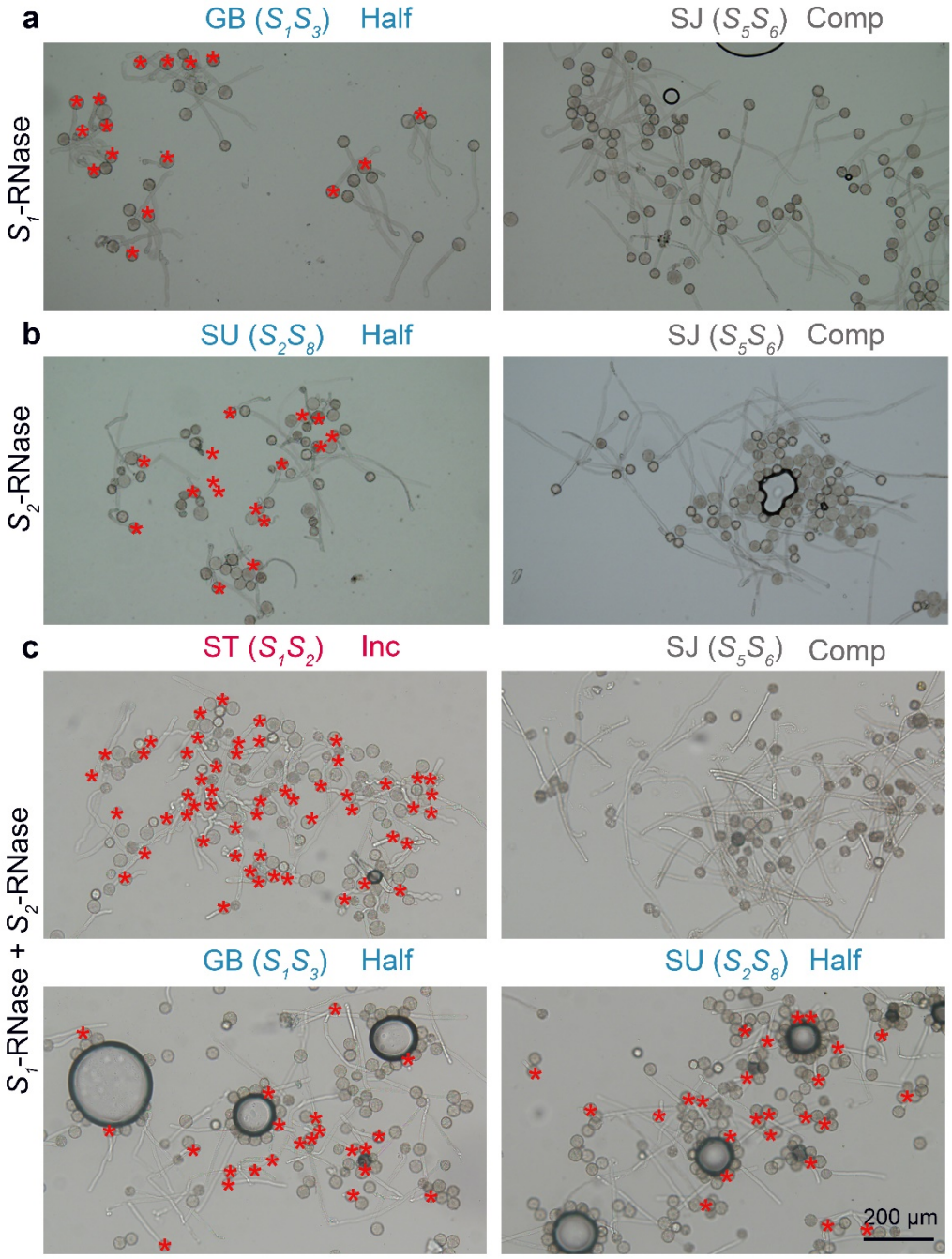

Supplementary Figure 9. Representative images of pummelo pollen tubes treated with recombinant *S*$_1$-RNase and *S*$_2$-RNase showing *S*-specific inhibitory activity.

a - c, Representative images of the effect of recombinant *S*$_1$-RNase (a), *S*$_2$-RNase (b) and *S*$_1$- + *S*$_2$-RNase (c) treatments (10 µg mL^{-1} per treatment) on pummelo pollen tube growth. For treatment of pollen with the *S*$_1$- or *S*$_2$-RNase separately, the outcomes are expected to be either half-compatible (half) where one *S*-allele is shared (e.g. for *S*$_1$*S*$_2$) or fully compatible (comp); where no *S*-alleles are shared (e.g. for pollen from plants carrying *S*$_5$*S*$_6$). Pollen tubes that were much shorter were judged to be inhibited (indicated by red asterisks). The accession name and *S*-genotype are indicated above each panel (e.g. accession ST has *S*-genotype *S*$_1$*S*$_2$). Each treatments was repeated independently three times with similar results.

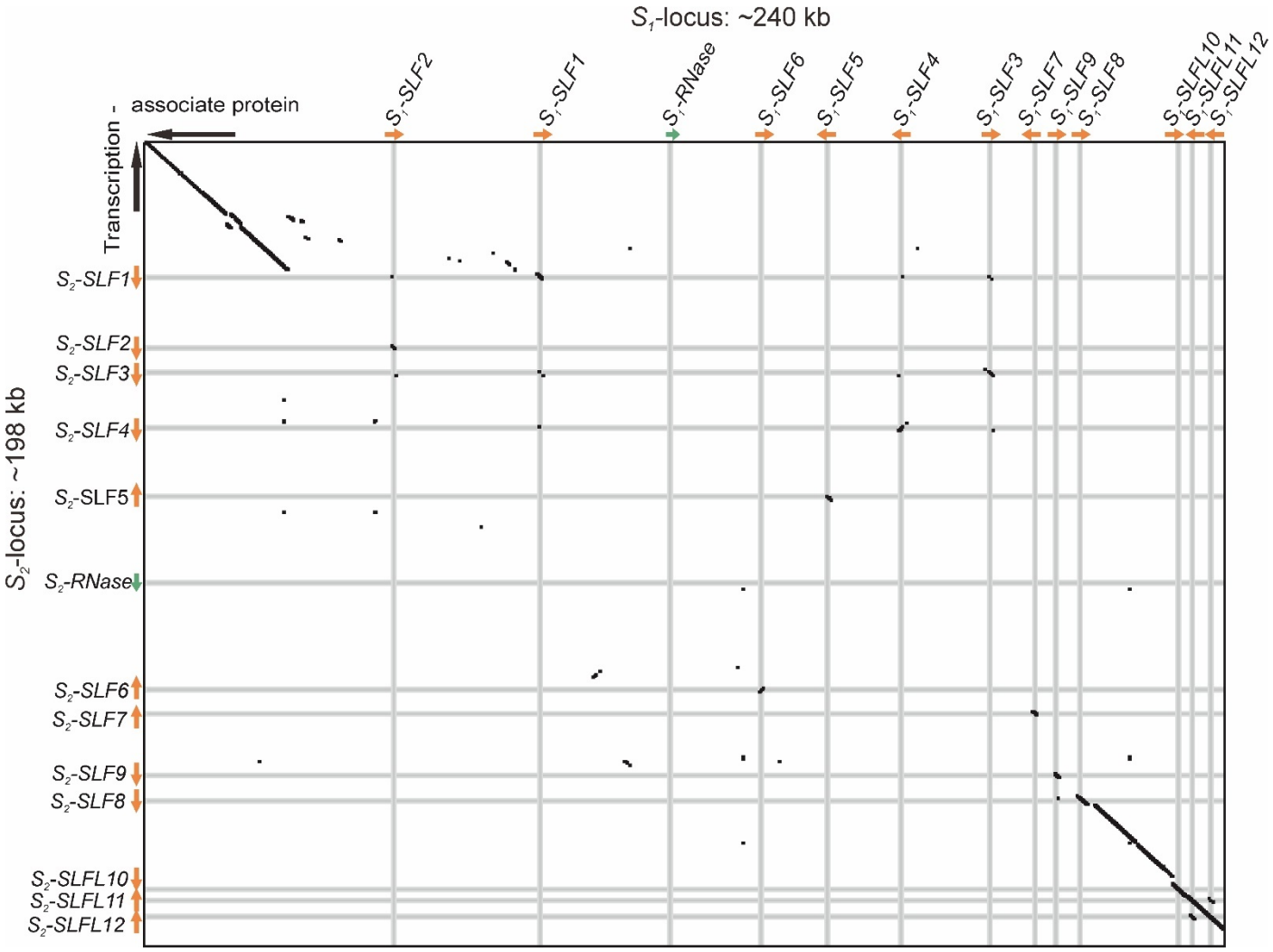

Supplementary Figure 10. Harr plot analysis between the pummelo *S1*-locus and the *S2*-locus.

Pattern matching analysis of homologies between DNA sequences (Harr plot analysis) between two pummelo *S*-loci (*S1* and *S2*). Each citrus *S*-locus contains a *S-RNase* and 12 candidate *SLF*s/*SLFL*s. The arrows indicate the direction of transcription for each gene.

The Harr plot was carried out by GENETYX Ver. 14 (GENETYX Corp., Tokyo, Japan) using the following settings: Unit size to compare: 8 bases; Cut off number: 22 bases; Minimum length: 25 bases.

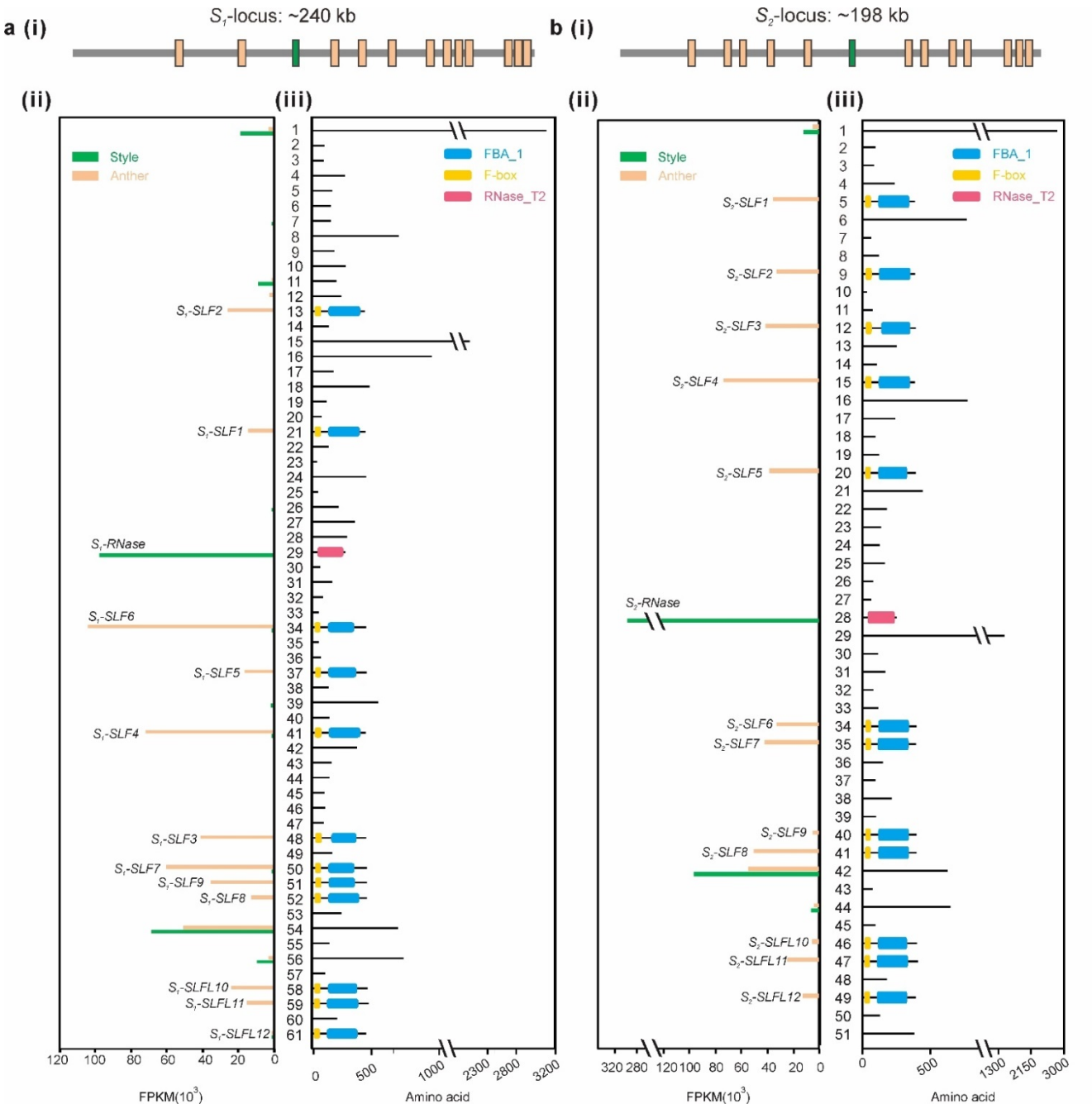

Supplementary Figure 11. The FPKM and conserved domains of *SLF/SLFL* genes located at the pummelo *S*$_1$- (a) and *S*$_2$-locus (b).

(i) Cartoon showing the overall structure of the *S*-loci. The relative positions of the *S-RNase* (green box) and the *F-box* (cream boxes) genes on the pummelo *S*-locus are shown, with the length of the *S*-locus indicated above.

(ii) FPKM values for the 61 genes on the pummelo *S*$_1$-locus (a) and 51 genes on the *S*$_2$-locus (b). FPKM was calculated with pair-end reads from anthers and styles 5 days before anthesis from *S*$_1$*S*$_3$ and *S*$_2$*S*$_5$ pummelo respectively. The pummelo *S-RNase* gene was specifically expressed in the style (green bar) and *SLF/SLFL* genes were specifically expressed in anthers (cream bars).

(iii) Schematic diagram of the relative positions of the conserved F-box, FBA_1 and RNase_T2 domains in predicted proteins present at the pummelo *S*$_1$-locus (a) and *S*$_2$-locus (b). These domains were predicted by the conserved domains database (CDD) at NCBI. Each *S*-locus has one *S-RNase* (with RNase _T2 domain, red block) and 12 *SLF*s/*SLFL*s, with F-box (yellow block) and FBA_1 domain (blue block).

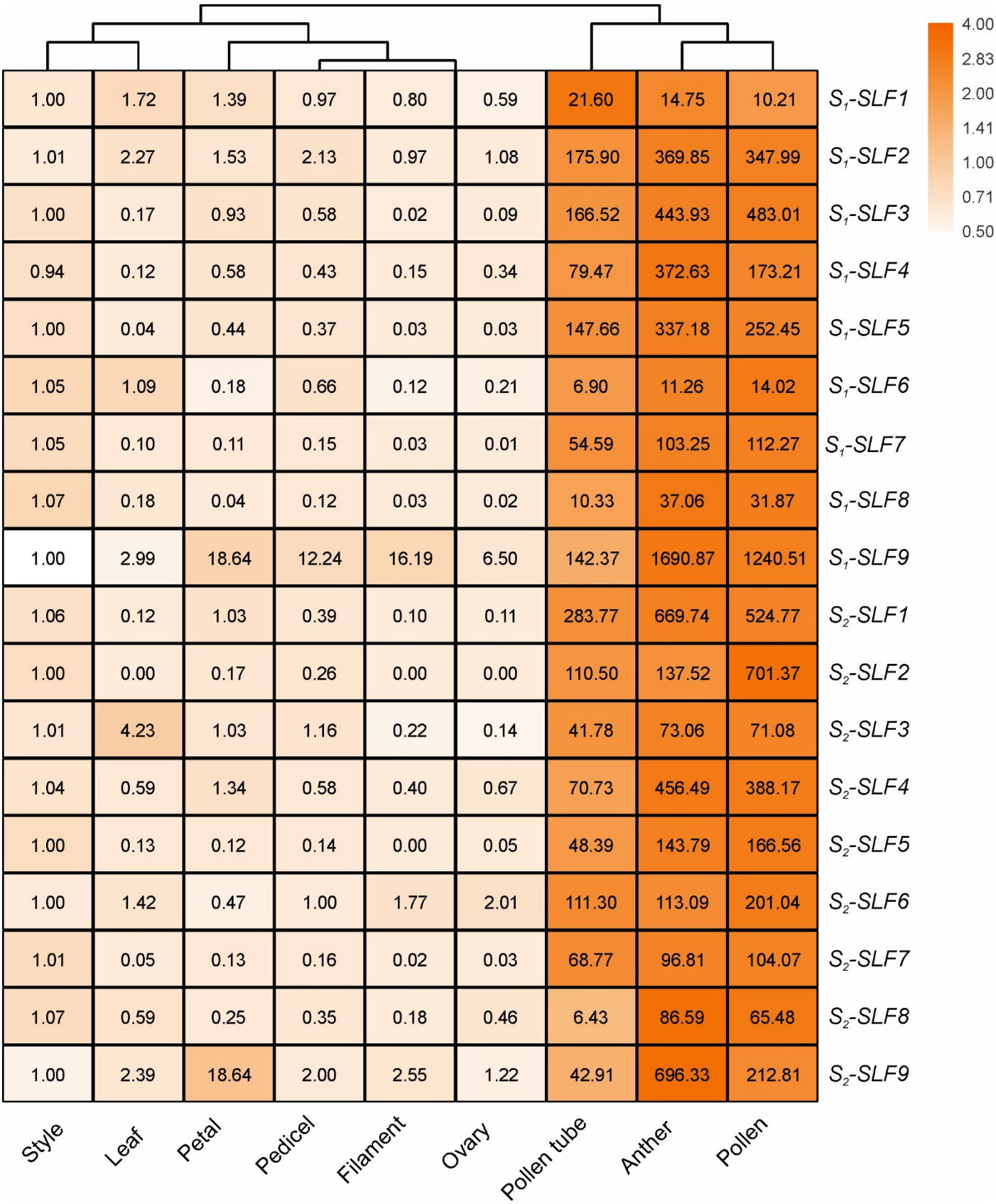

Supplementary Figure 12. Tissue-specific expression of pummelo *SLF* genes at the S_1- and S_2-loci.

Heat map showing the relative expression of *SLF* genes in different tissues from pummelo. All the tissues were obtained from a plant with a S_1S_2 genotype. The expression of each gene was quantified using qRT-PCR. The mean transcript levels (based on three biological replicates), is presented in each box. The scale bar on the right indicates the range of expression levels in $\log_2$-transformed values.

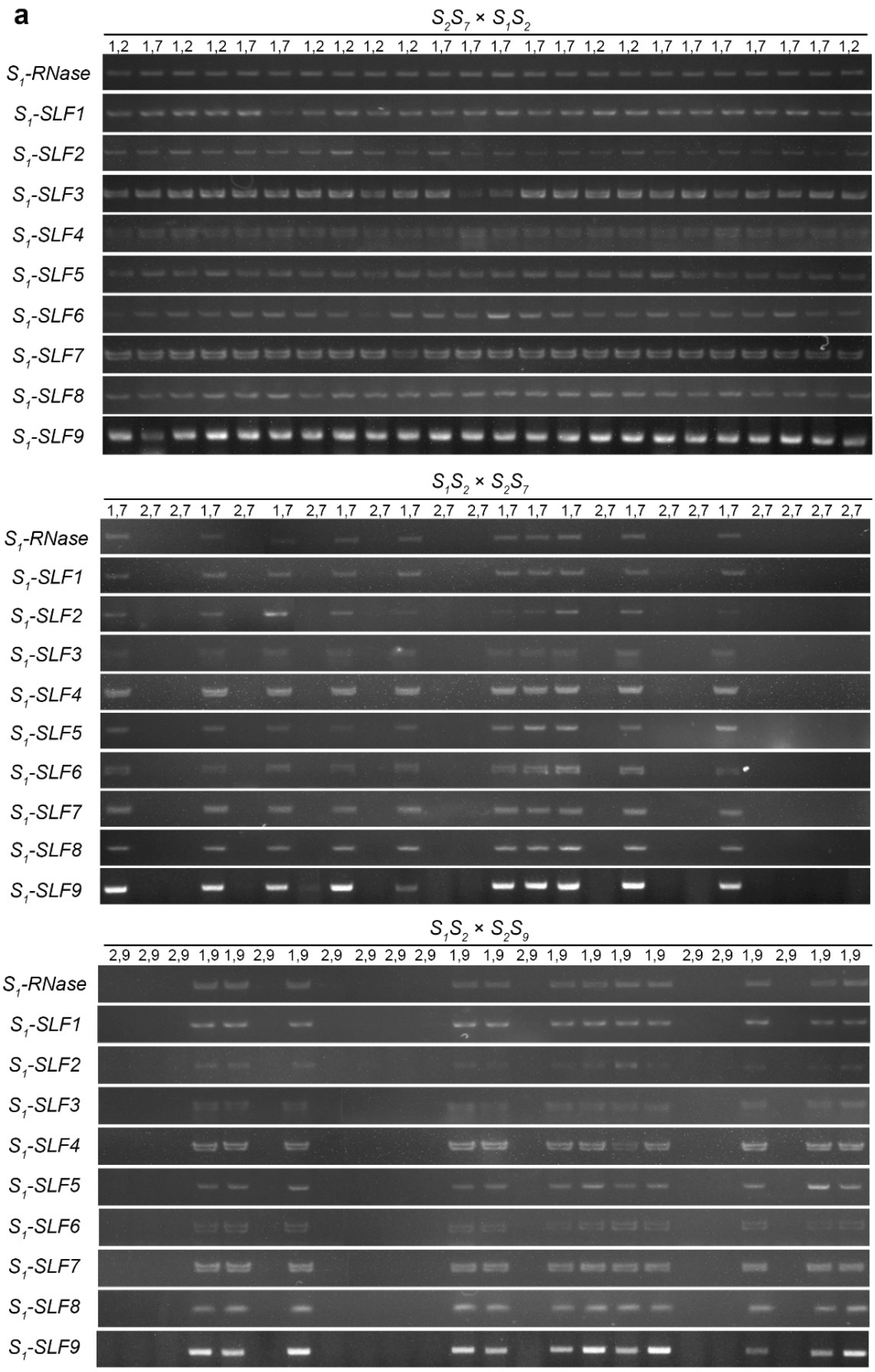
a
$S_2S_7 \times S_1S_2$
1,2 1,7 1,2 1,2 1,7 1,7 1,2 1,2 1,2 1,2 1,7 1,7 1,7 1,7 1,7 1,2 1,2 1,7 1,7 1,7 1,7 1,7 1,7 1,2
$S_1S_2 \times S_2S_7$
1,7 2,7 2,7 1,7 2,7 1,7 2,7 1,7 2,7 1,7 2,7 2,7 1,7 1,7 1,7 2,7 1,7 2,7 2,7 1,7 2,7 2,7 2,7 2,7
$S_1S_2 \times S_2S_9$
2,9 2,9 2,9 1,9 1,9 2,9 1,9 2,9 2,9 2,9 2,9 1,9 1,9 2,9 1,9 1,9 1,9 1,9 2,9 2,9 1,9 2,9 1,9 1,9
S_1-RNase
S_1-SLF1
S_1-SLF2
S_1-SLF3
S_1-SLF4
S_1-SLF5
S_1-SLF6
S_1-SLF7
S_1-SLF8
S_1-SLF9

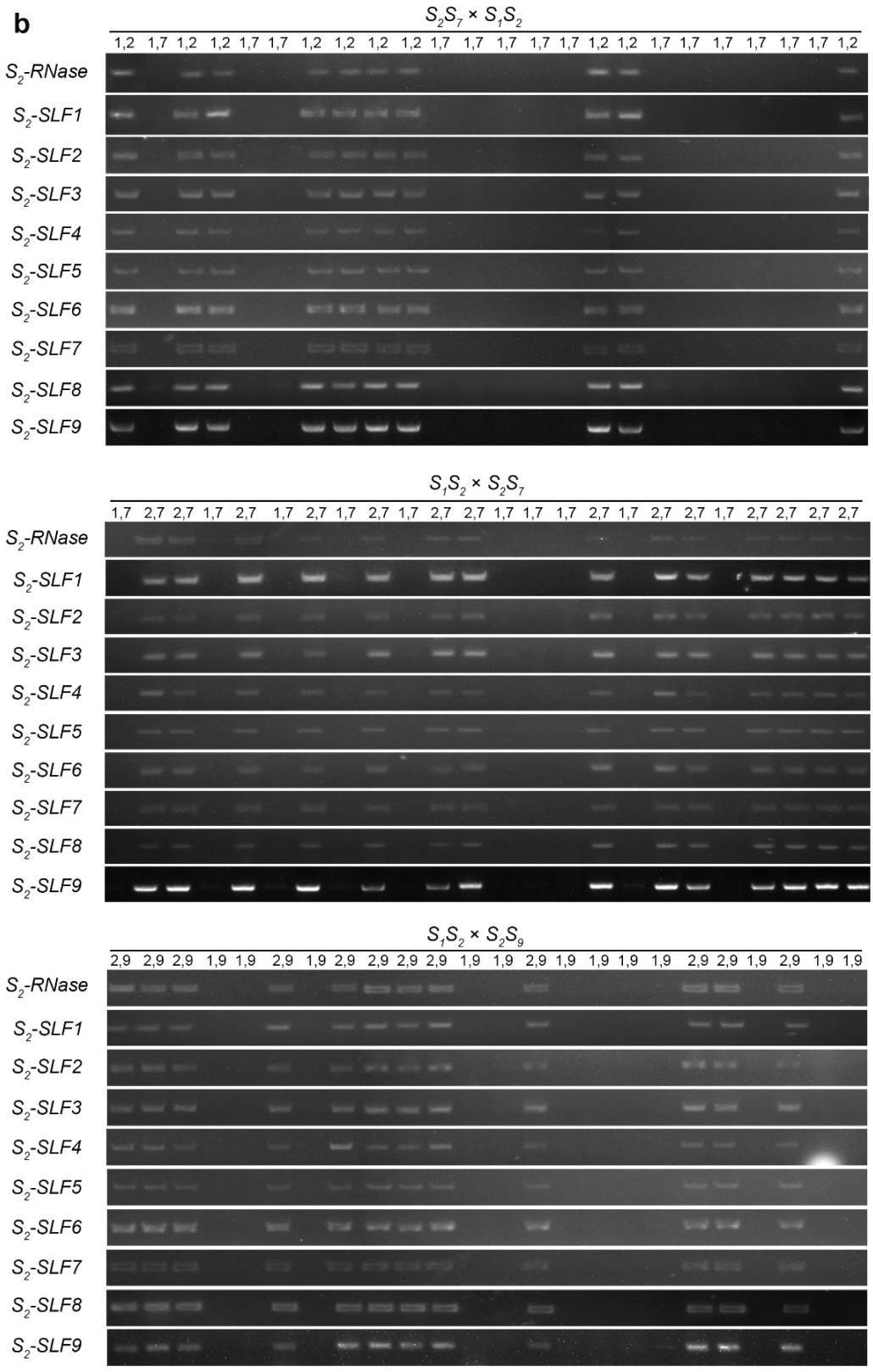

Supplementary Figure 13. Genetic linkage between pummelo *S-RNase* and *SLF*s in the S_1- (a) and S_2-loci (b).
Tissue from full-sibling pummelo families segregating for haplotypes (1) $S_2S_7 \times S_1S_2$, (2) $S_1S_2 \times S_2S_7$ and (3) $S_1S_2 \times S_2S_3$ was used for PCR, with each family containing 24 individuals.

(a) $SLF_{1\text{-}1}$ to $SLF_{1\text{-}9}$ were only amplified from plants carrying the S_1-allele and not those carrying S_2, S_7, S_9 alleles. **(b)** $SLF_{2\text{-}1}$ to $SLF_{2\text{-}9}$ were only amplified from plants carrying the S_2-allele and not those carrying S_1, S_7, S_9 alleles. These data show that all the pummelo *SLF*s are genetically linked to their cognate *S-RNase*. All of the genotypes were repeated independently two times with the same results.

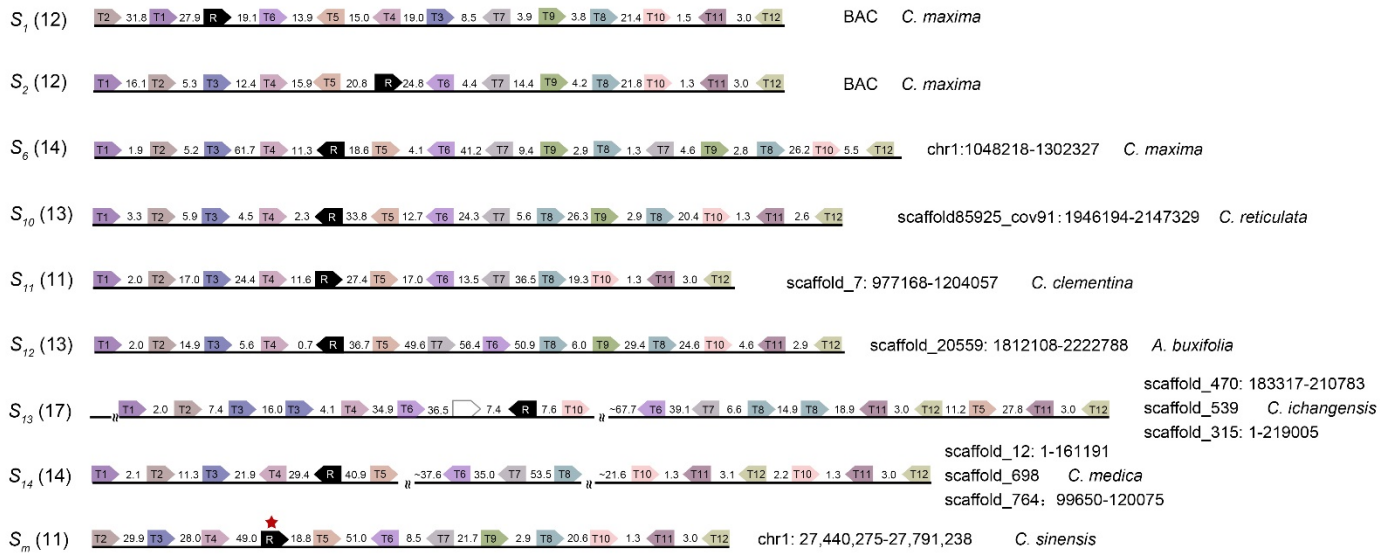

Supplementary Figure 14. Schematic diagram of the *S-RNase* and *SLF/SLFL* genes at the citrus *S*-loci.

Each citrus *S*-locus contains one *S-RNase* and multiple *SLF/SLFL* genes; the number of *SLF/SLFL* genes is indicated at the left of each *S*-locus in brackets. Genes are indicated with block arrows. The point of each block arrow indicates the direction of transcription. *S-RNase* genes are indicated with black arrows labeled with ‘‘R’’. *SLF/SLFL* genes are indicated with arrows labeled with “Tx”. The “x” indicates the type of *SLF/SLFL* gene. The 12 types of *SLF/SLFL* genes are indicated with different colors. *SLF/SLF* gene that belonged to none of the 12 types is indicated with white arrows without any labeling. The *S*-haplotype identified from the *C. maxima* genome was named S_6, because the *S-RNase* on the *S*-locus is identical to S_6-*RNase*. The *S*-haplotype identified from the *C. sinensis* genome was named S_m, because the *S-RNase* (red star) on the *S*-locus is mutated and encodes a truncated protein (see **Supplementary Fig. 11**). Note that the *S*-locus of *C. clementina* (S_{11}-locus) is located on scaffold 7, rather than scaffold 5 as previously reported[7].

S_1- and S_2-loci were screened from a BAC library. The other *S*-loci were obtained from available genome databases and their locations are indicated at the right of each *S*-locus. Because the assembly of the genome sequences of these species is incomplete and still at the scaffold stage, for the S_{13}- and S_{14}-loci. we obtained two and three fragments respectively, based on BLAST results (each conserved end has a homologous fragment, but the fragments have not been assembled together).

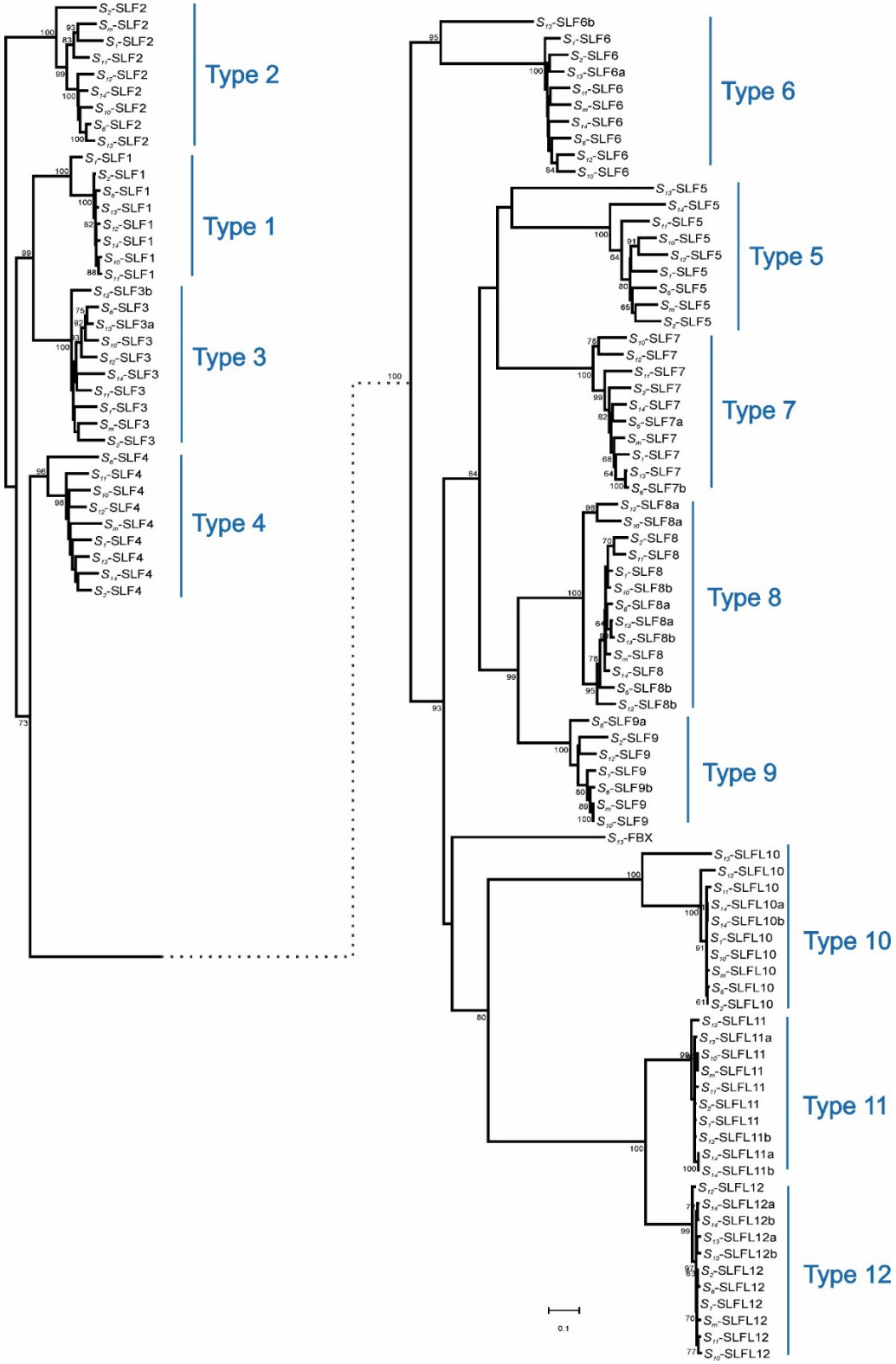

Supplementary Figure 15. Phylogeny of 117 *F-box* genes from nine *S*-loci from citrus.
Sequences of F-box proteins from different citrus species (*C. maxima*, *C. reticulata*, *C. clementina*, *C. sinensis*, *C. medica*, *C. ichangensis* and *A. buxifolia*) were analysed and grouped into 12 types based on their deduced amino acid sequences. They were named S_n-SLFx/S_n-SLFLx, according to the nomenclature used by Kubo et al.[8,9], with $_n$ and x indicating the *S*-haplotype and the type respectively. If two copies were present in one SLF type, they are indicated by a and b; e.g. S_{13}-SLF3a and S_{13}-SLF3b. The F-box that could not be grouped to the 12 types was named S_n-FBX, e.g. S_{13}-FBX. The allelic *SLFL*s within the type 10, 11 and 12 cluster grouped together on a very short branch.

Supplementary Figure 16. Deduced amino acid sequence alignments for the pummelo *S*$_1$-, *S*$_m$- and *S*$_m^R$-RNases.

The sequence of the pummelo *S*$_1$*-RNase*, (which has the highest homology to the *S*$_m$-RNase, 77% deduced amino acid identity, encodes 222 amino acid residues.

The natural mutant *S*$_m$*-RNase* gene has a stop codon at nucleotide position 498, resulting in a truncated coding sequence. The deduced amino acid sequence (166 residues) of *S*$_m$-RNase was, as expected, shorter than the unmutated *S*$_1$-RNases.

We engineered a "recovered" version (*S*$_m^R$-RNase) by inserting an adenine nucleotide at position 443 (red star, see **Supplementary Fig. 17**) in the truncated *S*$_m$*-RNase*. This resulted in the "recovered" *S*$_m^R$-RNase being extended to full length, equivalent to the normal *S*-RNase size, with a predicted transcript of 221 amino acids. The *S*$_m$-RNase has lost the hypervariable domains HV4 and HV5 and the conserved C4 and C5 domains.

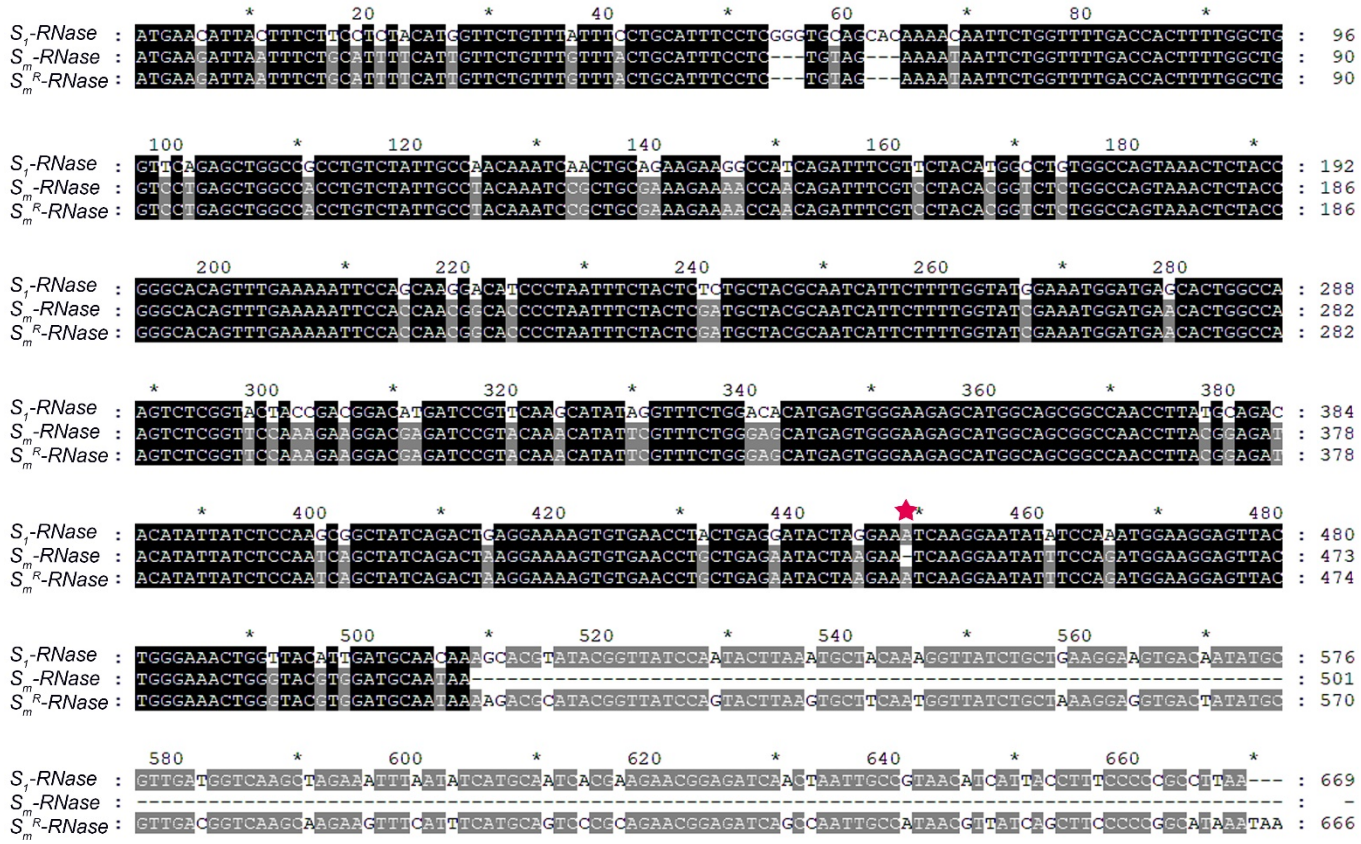

Supplementary Figure 17. Nucleotide sequence alignments of pummelo *S*$_1$-, *S*$_m$- and *S*$_m^R$-*RNase*.

To recover the function of the pummelo *S*$_m$-*RNase*, an adenine ("A", red star) nucleotide was introduced in *S*$_m^R$-*RNase* using the sequence of the *S*$_1$-*RNase*, which has the nearest sequence identity (~85% nucleotide identity) to the *S*$_m$/*S*$_m^R$-*RNase*, as a template.

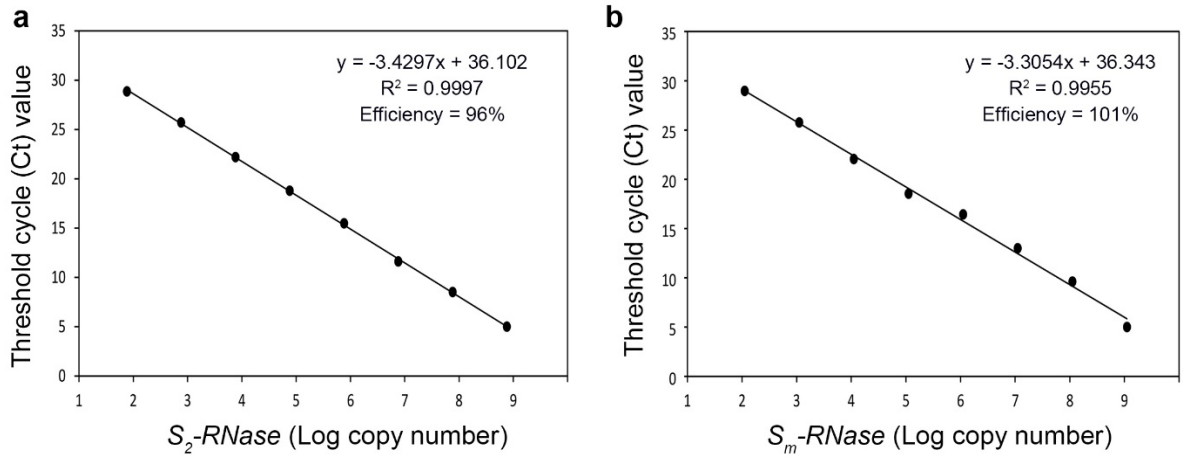

Supplementary Figure 18. Standard curves of the pummelo *S_2*- (a) and *S_m-RNase*s (b) generated by real-time PCR.

Because we used different primers to amplify the pummelo *S_2*- and *S_m-RNase*s, in order to be able to compare how their levels of expression compared, we needed to check that they had similar efficiencies. The Ct value over log copy number was plotted for the serial dilutions of input DNA templates. The efficiencies of the *S_2*- and *S_m-RNase* primers were calculated as described by Workenhe et al[10], showing that the *S_m*- and *S_2-RNase* primers have comparable amplification efficiencies. The equation of each regression line is shown; this was used to calculate the absolute copy number of *S_2*- and *S_m-RNase* in Figure 4c.

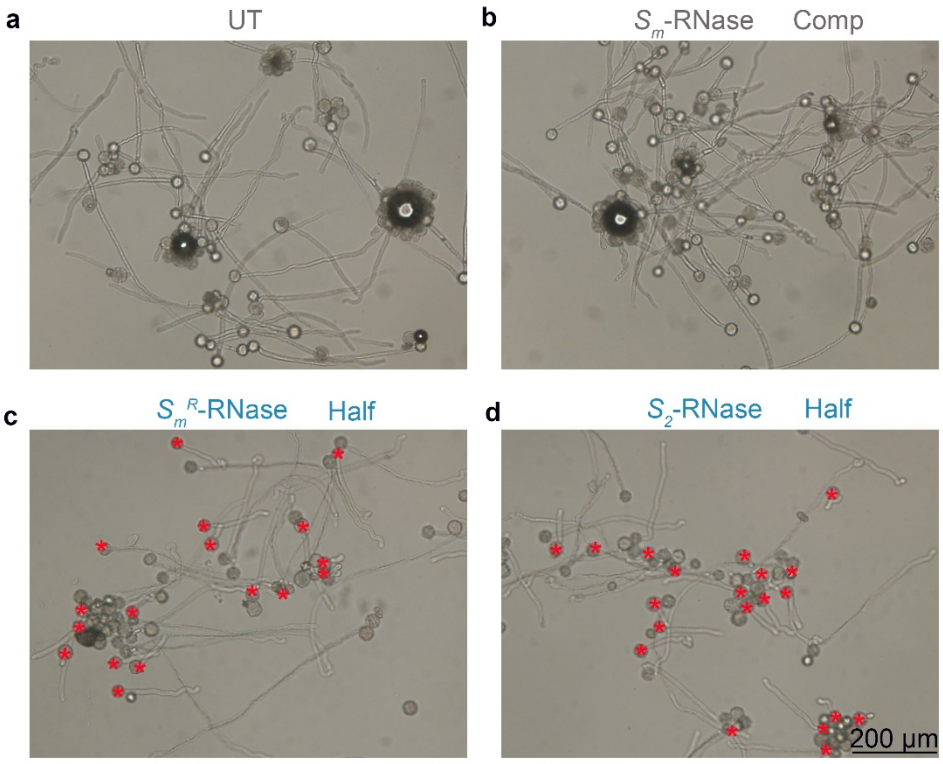

Supplementary Figure 19. Representative images of pummelo pollen tubes from a plant with the S_2S_m genotype growing in vitro after treatment with recombinant pummelo S_m-RNase, S_m^R-RNase or S_2-RNase.

(a) Untreated pollen (UT) had long pollen tubes.
(b) Pollen from a plant with the S_2S_m genotype was not inhibited by the mutant S_m-RNase protein.
(c) Pollen from a plant with the S_2S_m genotype had ~50% pollen tubes inhibited by the recombinant "recovered" S_m^R-RNase. This shows this recovered form has biological activity.
(d) Pollen from a plant with the S_2S_m genotype had ~50% pollen tubes inhibited by the recombinant S_2-RNase. This shows that the S_2 pollen is capable of being inhibited by cognate S_2-RNase.
This demonstrates the lack of pollen tube inhibitory activity of the mutant S_m-RNase protein and the *S*-specific inhibitory activity of the recovered S_m^R-RNase. Quantitation of these data are shown in Figure 4h.

Variant recombinant pummelo *S*-RNases (10 μg mL^{-1} per treatment) were added to pollen in the *in vitro* SI bioassay for 7 hours. All pollen was from a pummelo plant with the S_2S_m genotype (containing 50% S_m pollen and 50% S_2 pollen). For the sake of clarity, inhibited pollen tubes are indicated with red asterisks. Each treatments was repeated independently three times with similar results.

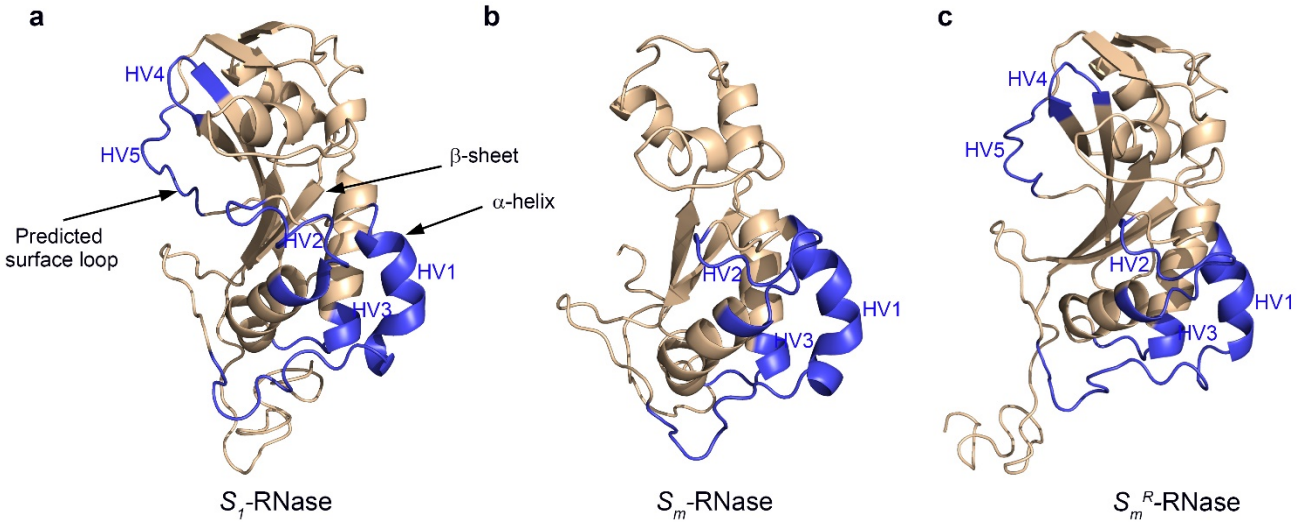

Supplementary Figure 20. Three-dimensional structural predictions of S_1- (a), S_m- (b) and S_m^R-RNase (c).

(a) The predicted 3D structure of the *S*-RNase (S_1-RNase) proteins has five hypervariable regions (in blue) and all of them are predicted to reside at the surface of the protein.

(b) The predicted 3D structure of the mutant S_m-RNase. The HV4 and HV5 domains are missing.

(c) The predicted 3D structure of the "recovered" S_m^R-RNase is (as expected) similar to that of S_1-RNase with five hypervariable regions.

The predicted 3D structure of the *S*-RNases (S_1-RNase and S_m^R-RNase) comprises six α-helices and six β-sheets. The hypervariable regions (HV1-HV5) are labelled in blue. Comparisons of these structural predictions (and with published *S*-RNase structural predictions from *Nicotiana*, which implicate HVa and HVb in recognition as they are within surface loops)[11], suggest that the pummelo hypervariable domains HV4 and HV5, which are also predicted to reside at the surface of the protein may be involved in *S*-specific recognition, as the mutant S_m-RNase is defective: retaining RNase activity, but lacking pollen inhibitory activity).

The structural predictions were carried out using I-TASSER server; see Methods for details.

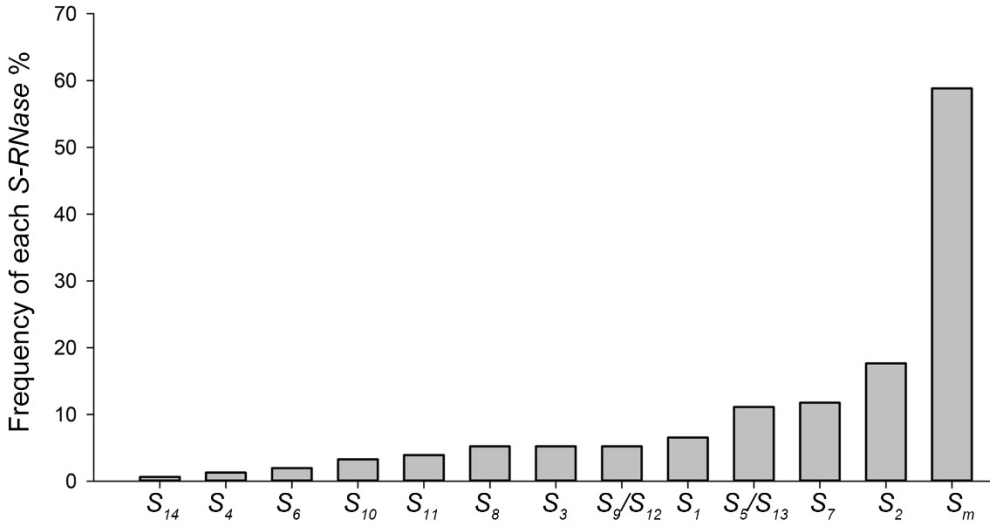

Supplementary Figure 21. Frequency of *S-RNase* genes in 153 citrus accessions.

All of the *S-RNase*s showed evidence of negative frequency dependent selection, with a low occurrence in the 153 citrus accessions examined. This pattern of distribution was also observed in 391 pummelo accessions (see **Supplementary Fig. 5b**). In contrast, the mutant S_m-*RNase* has a high occurrence (58.8% frequency) in the citrus accessions, which conflicts with it being controlled by negative frequency dependence.

Short read mapping failed to distinguish the S_9-*RNase* and S_{12}-*RNase* pairs of genes and those of the S_5-*RNase* and S_{13}-*RNase* because their sequences were similar. Thus, the bars of S_9/S_{12} and S_5/S_{13} represent the frequencies of both S_9-*RNase* and S_{12}-*RNase* and both S_5-*RNase* and S_{13}-*RNase*, respectively.

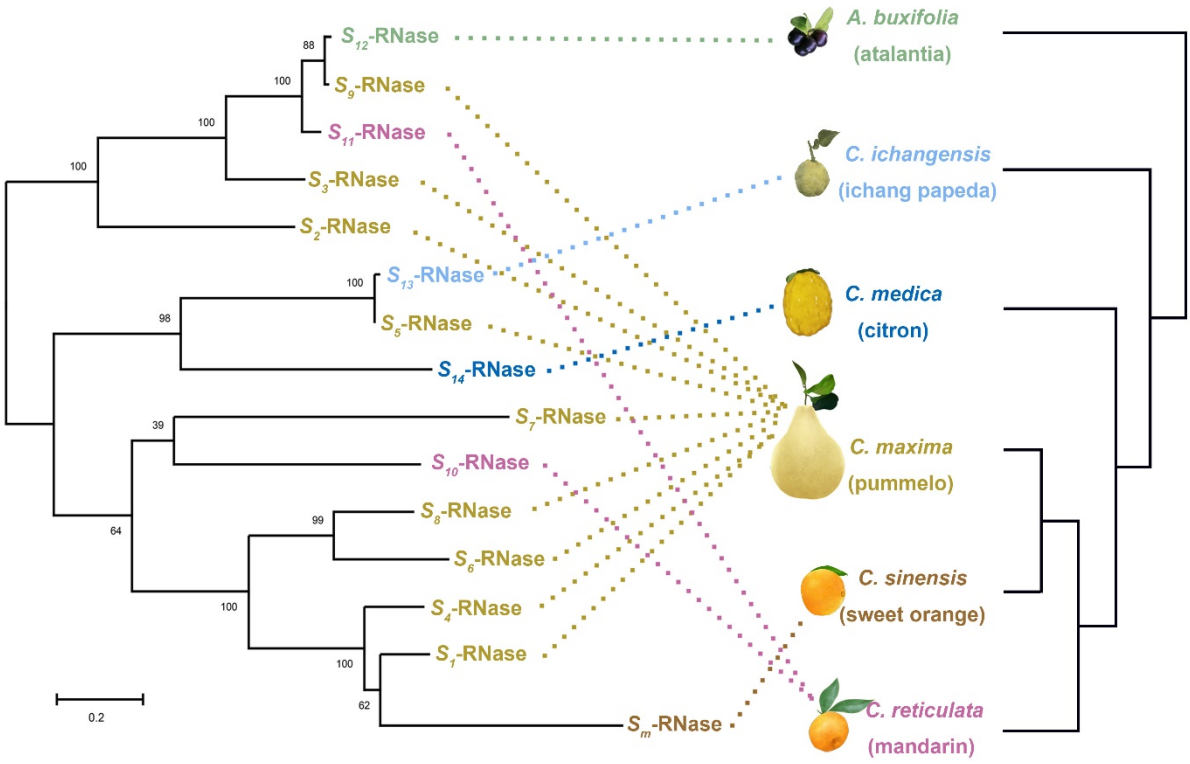

Supplementary Figure 22. Phylogeny of 15 *S*-RNases from citrus varieties.

We put the phylogenetic tree for the citrus *S-RNase*s together with the phylogenic tree of the citrus species, as described by Wang et al[12]. The different coloured text indicates the *S*-RNase from different citrus species. The phylogeny of the *S-RNase*s was inconsistent with the phylogeny of citrus species. This suggests that the *S*-RNases are either older than the formation of these accessions or that the divergence of these *S*-RNases is earlier than citrus divergence.

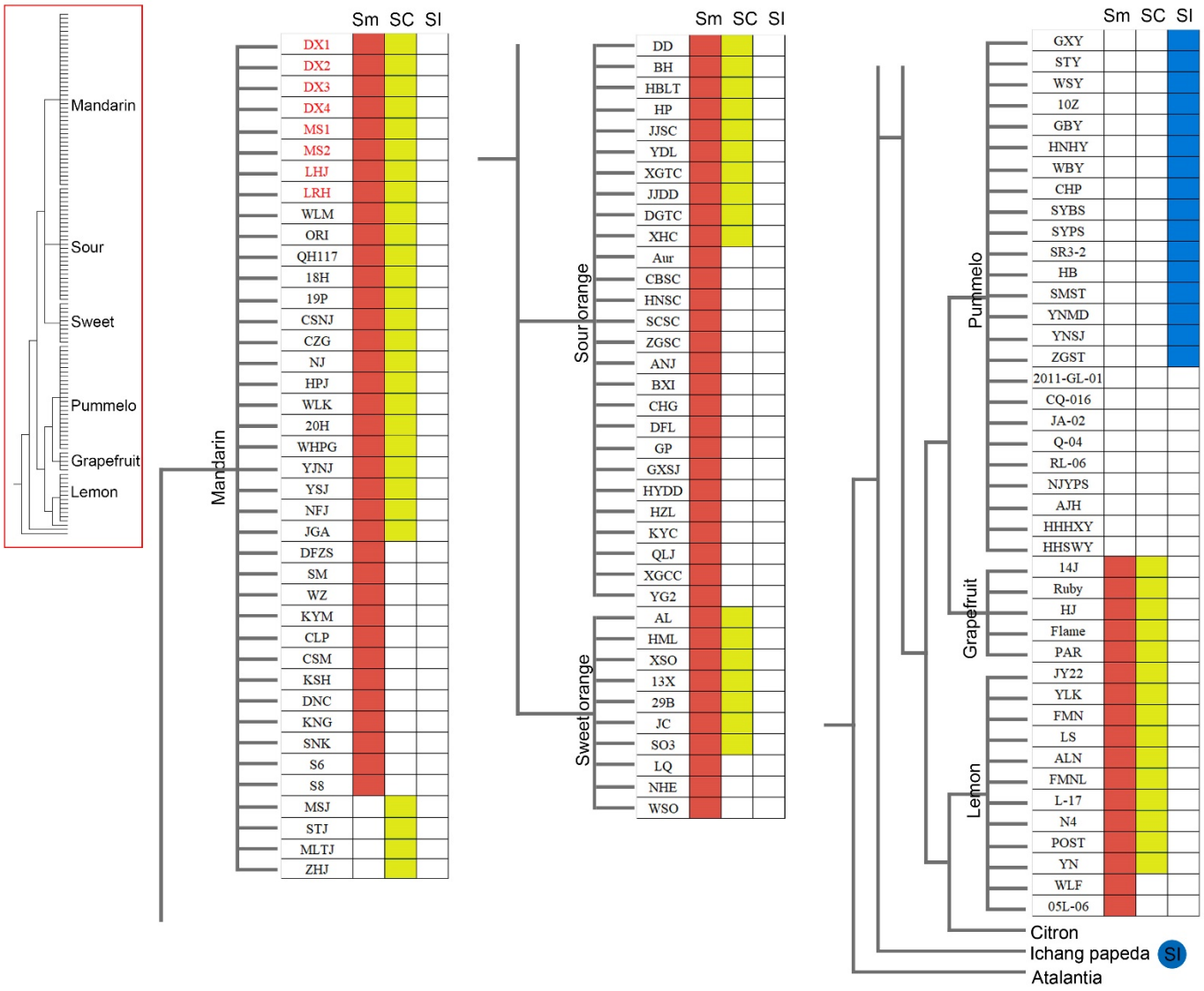

Supplementary Figure 23. A tree illustration of the conservation of the *S_m-RNase* in citrus accessions.

The phylogenic tree was drawn as described by Wang et al[12]. The main figure shows an expansion of the tree shown on the far left.

Ninety out of the 153 citrus accessions possess the *S_m-RNase* (red block), of which the self-compatibility of 56 accessions (>60%, yellow block) was demonstrated using aniline blue staining. Several accessions (MSJ, STJ, MLTJ and ZHJ) were self-compatible, but they did not have the *S_m-RNase*, suggesting that the disruptive *S_m-RNase* is the primary mutation responsible for the SC phenotype in citrus, but that it is not the only mutation. The *S_m-RNase* was not present in the self-incompatible accessions (blue blocks). *Ichang papeda*, which is self-incompatible (blue circle; see **Supplementary Fig. 23)**, is an ancestral species, as shown in the tree. The wild mandarin accessions are indicated in red font.

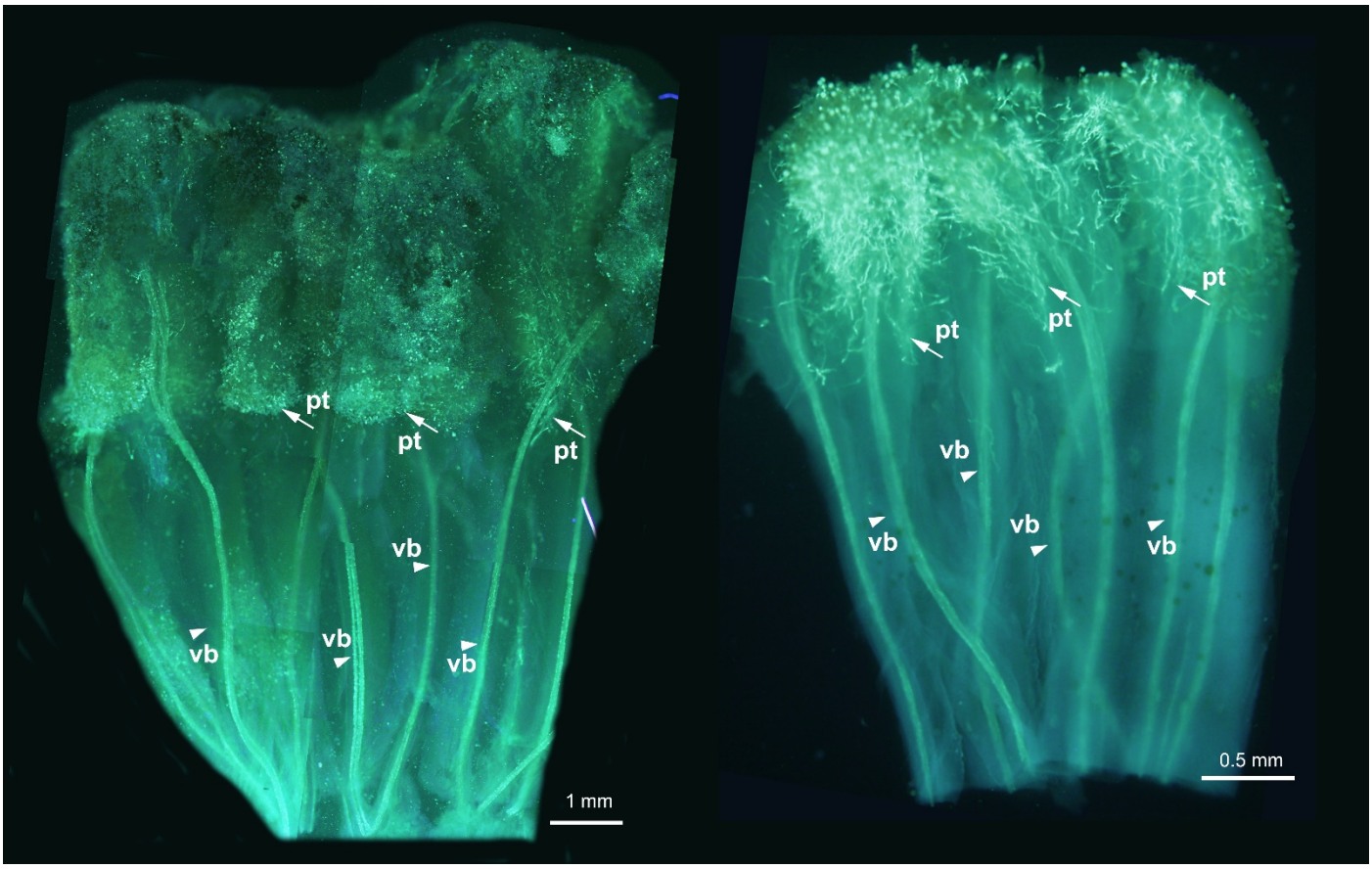

Supplementary Figure 24. Evidence that *Ichang papeda* is self-incompatible.

Representative aniline blue staining of self-pollinated styles from two *Ichang papeda* accessions collected from different provinces. Five pollinations from each accession were examined. The pollen tubes of both of them were inhibited near the top of the style, which is a SI phenotype. Pollen tubes (pt) are indicated with arrows; vascular bundles (vb) are indicated with arrowheads. At least five self-pollinated pistils of the two accessions were observed.

Supplementary Table 1. Overview of the pummelo accessions used in the pollinations in this study

No.	Accession name	Common name	Species	Scientific name [a]	Harvest place of the samples
1	ST	Shatian pummelo	Pummelo	*C. maxima*	Guilin City, Guangxi, China
2	SU	Sour pummelo	Pummelo	*C. maxima*	Guilin City, Guangxi, China
3	SJ	Shuijing pummelo	Pummelo	*C. maxima*	Dehong City, Yunnan, China
4	GX	Guanximiyou pummelo	Pummelo	*C. maxima*	Dehong City, Yunnan, China
5	MD	Burma pummelo	Pummelo	*C. maxima*	Dehong City, Yunnan, China
6	WS	Acidless pummelo	Pummelo	*C. maxima*	Dehong City, Yunnan, China
7	WB	Wanbai pummelo	Pummelo	*C. maxima*	Wuhan City, Hubei, China
8	GB	Gaoban pummelo	Pummelo	*C. maxima*	Wuhan City, Hubei, China
9	HB	HB pummelo	Pummelo	*C. maxima*	Wuhan City, Hubei, China
10	HN	Huanong red pummelo	Pummelo	*C. maxima*	Wuhan City, Hubei, China
11	ZP	Purple pummelo	Pummelo	*C. maxima*	Wuhan City, Hubei, China
12	TG	Thailand acidless ummelo	Pummelo	*C. maxima*	Wuhan City, Hubei, China
13	SM	Shimengshatian pummelo	Pummelo	*C. maxima*	Changde City, Hubei, China
14	ZG	Ziguishatian pummelo	Pummelo	*C. maxima*	Yichang City, Hubei, China
15	CL	Cilitian pummelo	Pummelo	*C. maxima*	Changsha City, Hunan, China

[a]: The names *C. maxima* and *C. grandis* are both currently used for pummelo. As *C. maxima* is adopted under the International Code of Botanical Nomenclature, we use *C. maxima* throughout.

Supplementary Table 2. Fruit set and seed number of self- and cross-pollinations between different pummelos (*C. maxima*)

♀/♂		GB S_1S_3	HB S_2S_7	WB S_2S_5	SJ S_5S_6	GX S_8S_9	MD S_3S_5	ST S_1S_2	SU S_2S_8	WS S_2S_4	Unpollinated
GB S_1S_3	**Fruit set ratio (%)**[a]	0.00	22.45	23.26	39.39	21.88	30.95	21.62	27.27	33.33	0.00
	Seeds per fruit[b]	0	183±12	165±12	152±17	132±14	172±8	145±25	149±11	158±10	0
HB S_2S_7	**Fruit set ratio (%)**		3.03	23.33	34.00	47.06	40.35	77.36	60.53	43.18	5.26[c]
	Seeds per fruit		0	87±12	94±5	97±15	101±5	93±11	88±9	66±7	0
WB S_2S_5	**Fruit set ratio (%)**			12.12	54.55	8.70	41.18	42.86	18.60	17.95	6.06[c]
	Seeds per fruit			0	77±4	68±15	92±6	61±3	83±8	90±5	0
SJ S_5S_6	**Fruit set ratio (%)**				30.77	67.92	81.36	36.07	57.35	43.06	12.90[c]
	Seeds per fruit				0	179±11	197±3	142±32	183±22	221±21	0
GX S_8S_9	**Fruit set ratio (%)**					60.00	53.85	82.35	75.00	33.33	21.21[c]
	Seeds per fruit					0	120±11	110±9	108±9	111±6	0
MD S_3S_5	**Fruit set ratio (%)**						0.00	20.97	25.40	5.66	0.00
	Seeds per fruit						0	127±14	128±10	101±29	0
ST S_1S_2	**Fruit set ratio (%)**							0.00	9.26	6.00	0.00
	Seeds per fruit							0	67±10	104±17	0
SU S_2S_8	**Fruit set ratio (%)**								0.00	16.67	0.00
	Seeds per fruit								0	96±6	0
WS S_2S_4	**Fruit set ratio (%)**									0.00	0.00
	Seeds per fruit									0	0

Self- and cross-pollinations between different pummelos (*C. maxima*) were performed. Fruit set and seed number established that these accessions were self-incompatible. Unpollinated flowers were also assessed and established several parthenocarpic accessions.

Fruit set ratios varied due to different climate and cultivation techniques in sampled provinces.

[a] : Fruit set ratio = Number of fruit/pollinated flowers*100.

[b] : The seeds per fruit value is shown in mean ± SEM (n > 5).

[c] : The non-zero fruit set ratio for non-pollination indicates that this accession is characterized by parthenocarpy.

Supplementary Table 3. Detailed information relating to data from citrus style and anther RNA-seq libraries.

Species (*S*-genotype)	Sample name [a]	Tissue [b]	Number of read pairs	Clean bases (G)	Read length (bp)	GC (%)	SRR id in GenBank
Sour pummelo (S_2S_8)	SU_A1_1	Anther from -1 DBA	34986795	10.50	150	44.63	SRR8862738
	SU_A1_2		47440832	14.23	150	44.73	SRR8862737
	SU_S1_1	Style from -1 DBA	49400601	14.82	150	43.29	SRR8862740
	SU_S1_2		46643336	13.99	150	43.34	SRR8862739
	SU_S3_1	Style from -3 DBA	46429691	13.93	150	43.86	SRR8862742
	SU_S3_2		49569693	14.87	150	44.37	SRR8862741
	SU_S5_1	Style from -5 DBA	34592510	10.38	150	44.54	SRR8862744
	SU_S5_2		38624135	11.59	150	44.26	SRR8862743
Shuijing pummelo (S_5S_6)	SJ_A_1	Anther from -1 DBA	35650637	10.70	150	44.68	SRR8862889
	SJ_A_2		49096449	14.73	150	45.24	SRR8862888
	SJ_S1_1	Style from -1 DBA	48395409	14.52	150	44.20	SRR8862891
	SJ_S1_2		57505312	17.25	150	44.18	SRR8862890
	SJ_S3_1	Style from -3 DBA	60446005	18.13	150	44.43	SRR8862893
	SJ_S3_2		48320149	14.50	150	44.83	SRR8862892
	SJ_S5_1	Style from -5 DBA	35372692	10.61	150	44.88	SRR8862895
	SJ_S5_2		56603062	16.98	150	44.17	SRR8862894
Guanximiyou pummelo (S_8S_9)	GX_A_1	Anther from -1 DBA	35249007	10.57	150	44.18	SRR8863082
	GX_A_2		47088015	14.13	150	44.56	SRR8863081
	GX_S1_1	Style from -1 DBA	54147780	16.24	150	43.87	SRR8863080
	GX_S1_2		51849281	15.55	150	44.53	SRR8863079
	GX_S3_1	Style from -3 DBA	42133229	12.64	150	44.42	SRR8863078
	GX_S3_2		49961516	14.99	150	44.52	SRR8863077
	GX_S5_1	Style from -5 DBA	34985907	10.50	150	44.38	SRR8863076
	GX_S5_2		47723135	14.32	150	44.96	SRR8863075
Burma pummelo (S_3S_5)	MD_A1_1	Anther from -1 DBA	35202890	10.56	150	44.52	SRR8863197
	MD_A1_2		40000748	12.00	150	44.89	SRR8863198
	MD_S1_1	Style from -1 DBA	46929628	14.08	150	43.17	SRR8863195
	MD_S1_2		50304716	15.09	150	43.39	SRR8863196
	MD_S3_1	Style from -3 DBA	48058900	14.42	150	44.20	SRR8863201
	MD_S3_2		42769012	12.83	150	44.26	SRR8863202
	MD_S5_1	Style from -5 DBA	35605996	10.68	150	44.36	SRR8863199
	MD_S5_2		38898539	11.67	150	44.49	SRR8863200
Acidless pummelo (S_2S_4)	WS_A_1	Anther from -1 DBA	35131284	10.54	150	44.45	SRR9124567
	WS_A_2		48123801	14.44	150	45.32	SRR9124568
	WS_S1_1	Style from -1 DBA	42166068	12.65	150	44.40	SRR9124569
	WS_S1_2		50294489	15.09	150	44.15	SRR9124570

Acidless pummelo (S_2S_4)	WS_S3_1	Style from -3 DBA	51303398	15.39	150	44.36	SRR9124563
	WS_S3_2		53274604	15.98	150	44.31	SRR9124564
	WS_S5_1	Style from -5 DBA	35225241	10.57	150	44.51	SRR9124565
	WS_S5_2		54403425	16.32	150	44.45	SRR9124566
Wanbai pummelo (S_2S_5)	WB_A_1	Anther from -1 DBA	34958874	10.49	150	44.59	SRR8868189
	WB_A_2		45894467	13.77	150	45.41	SRR8868188
	WB_S1_1	Style from -1 DBA	46744496	14.02	150	43.73	SRR8868191
	WB_S1_2		43126224	12.94	150	44.27	SRR8868190
	WB_S3_1	Style from -3 DBA	57056644	17.12	150	43.49	SRR8868193
	WB_S3_2		44779195	13.43	150	44.30	SRR8868192
	WB_S5_1	Style from -5 DBA	34476290	10.34	150	44.47	SRR8868195
	WB_S5_2		49019973	14.71	150	45.10	SRR8868194
Gaoban pummelo (S_1S_3)	GB_A_1	Anther from -1 DBA	35134343	10.54	150	44.35	SRR8872464
	GB_A_2		48866759	14.66	150	44.65	SRR8872465
	GB_S1_1	Style from -1 DBA	47323297	14.20	150	44.05	SRR8872462
	GB_S1_2		54437906	16.33	150	43.91	SRR8872463
	GB_S3_1	Style from -3 DBA	47402934	14.22	150	44.15	SRR8872468
	GB_S3_2		43047147	12.91	150	44.07	SRR8872469
	GB_S5_1	Style from -5 DBA	35295439	10.59	150	44.41	SRR8872466
	GB_S5_2		52479355	15.74	150	44.25	SRR8872467
HB pummelo (S_2S_7)	HB_A_1	Anther from -1 DBA	34354387	10.31	150	44.73	SRR8873603
	HB_A_2		37430244	11.23	150	45.16	SRR8873602
	HB_S1_1	Style from -1 DBA	48755530	14.63	150	44.65	SRR8873601
	HB_S1_2		45563444	13.67	150	44.63	SRR8873600
	HB_S3_1	Style from -3 DBA	48163285	14.45	150	44.90	SRR8873607
	HB_S3_2		52484687	15.75	150	44.80	SRR8873606
	HB_S5_1	Style from -5 DBA	34936798	10.48	150	44.45	SRR8873605
	HB_S5_2		53906104	16.17	150	44.29	SRR8873604
Cocktail grapefruit (S_2S_m)	JW_A_1	Anther	39652164	11.90	150	44.18	SRR10168371
	JW_A_2		39805971	11.94	150	44.48	SRR10168370
	JW_S_1	Style	40976310	12.29	150	44.49	SRR10168370
	JW_S_2		44653340	13.40	150	44.50	SRR10168368

Data from 68 RNA-seq libraries of style and anther from eight pummelos and one grapefruit.. Nine candidate *S-RNase* genes with complete open reading frames (ORFs) were identified.

[a]: Sample name is designate as A-B-C, with A indicating the accession code (**Supplementary Table 1**), B indicates the tissue, C indicates the repetition.

[b]: -1, -2, -3, -4 and -5 DBA represents 1, 2, 3, 4, and 5 days before anthesis.

Supplementary Table 4. Predicted Mrs and IEFs for *S*-RNases from the Rutaceae with reference to those in the Plantaginaceae, Solanaceae, and Rosaceae.

Gene	Organism	Full length	Amino acid	Molecular mass (kDa) [a]	Isoelectric point [a]	Source	Accession number
S_1-RNase	*C. maxima*	669	222	23.38	8.23	In this study	MN652897
S_2-RNase	*C. maxima*	699	232	24.17	9.22	In this study	MN652898
S_3-RNase	*C. maxima*	696	231	24.06	9.11	In this study	MN652899
S_4-RNase	*C. maxima*	675	224	23.16	8.84	In this study	MN652900
S_5-RNase	*C. maxima*	660	219	23.16	7.71	In this study	MN652901
S_6-RNase	*C. maxima*	660	219	22.96	9.39	In this study	MN652902
S_7-RNase	*C. maxima*	696	231	24.02	8.93	In this study	MN652903
S_8-RNase	*C. maxima*	690	229	24.47	7.67	In this study	MN652904
S_9-RNase	*C. maxima*	690	229	24.10	9.33	In this study	MN652905
S_{10}-RNase	*C. reticulata*	690	229	24.02	9.12	In this study	MN652906
S_{11}-RNase	*C. reticulata*	690	229	24.08	9.47	In this study	MN652907
S_{12}-RNase	*A. buxifolia*	690	229	24.25	9.30	In this study	MN652908
S_{13}-RNase	*C. ichangensis*	660	219	23.22	7.71	In this study	MN652909
S_{14}-RNase	*C. medica*	678	225	22.91	8.27	In this study	MN652910
S_m-RNase	*C. sinensis*	501	166	17.47	7.24	In this study	MN652911
S_m^R-RNase	*C. sinensis*	666	221	23.59	8.23	In this study	MN652912
S_5-RNase	*Antirrhinum hispanicum*	702	233	23.83	9.01	Xue et al, 1996[13]	X96464
S_7-RNase	*Petunia x hybrida*	657	218	23.08	8.32	Kubo et al, 2010[8]	AB568388
Sc-RNase	*Malus spectabilis*	672	223	22.97	9.13	Ushijima et al, 1998[14,15]	FJ943264

[a]: The molecular mass and the isoelectric point of the *S*-RNases were predicted using the mature protein sequence without the signal peptide.

All of the *S*-RNases from the Rutaceae have a similar full length (~ 660 bp) coding region, amino acid number (~ 220), molecular weight (~ 24 kDa) and basic isoelectric point. They are similar to the characteristics of sample *S*-RNases from the Plantaginaceae, Solanaceae, and Rosaceae (indicated in blue). *S*-RNases differ from other RNases in having unusually high isoelectric points, which is a key characteristic of these proteins.

Supplementary Table 5. Compatibility relationships between different pummelo accessions, as assigned by aniline blue staining.

♀/♂	ST *S_1S_2*	GB *S_1S_3*	SM *S_1S_3*	WS *S_2S_4*	TG *S_2S_4*	WB *S_2S_5*	MD *S_3S_5*	ZP *S_3S_5*	ZG *S_3S_5*	SJ *S_5S_6*	HB *S_2S_7*	CL *S_1S_7*	HN *S_1S_8*	SU *S_2S_8*	GX *S_8S_9*
ST *S_1S_2*	--(5/5)			+(2/3) ++(1/3)		+(2/4) ++(2/4)	++(3/3)			++(5/5)	+(2/2)			+(4/4)	++(4/4)
GB *S_1S_3*	+(3/4) ++(1/4)	--(10/10)	--(12/12)	++(7/7)		++(3/3)	+(5/6) ++(1/6)			++(4/4)	++(5/5)		+(3/5) ++(2/5)	++(8/8)	++(9/9)
SM *S_1S_3*			--(3/3)												
WS *S_2S_4*	+(4/5) ++(1/5)	++(6/6)		--(3/3)	--(6/6)	+(3/4) ++(1/4)	++(3/3)	++(7/7)		++(6/6)	+(3/3)		++(6/6)	+(5/6) ++(1/6)	++(4/4)
TG *S_2S_4*					--(4/4)										
WB *S_2S_5*	+(3/3)	++(5/5)		+(3/3)		--(4/4)	+(1/3) ++(2/3)	+(10/15) ++(5/15)		+(4/5) ++(1/5)	+(3/3)		++(2/2)	+(1/2) ++(1/2)	++(5/5)
MD *S_3S_5*	++(2/2)			++(10/10)		+(2/5) ++(3/5)	--(11/11)			+(2/4) ++(2/4)	++(2/2)			++(6/6)	++(9/9)
ZP *S_3S_5*	++(5/5)	+(3/5) ++(2/5)		++(5/5)		+(5/6) ++(1/6)	--(17/17)	--(14/14)	--(4/4)	+(4/6) ++(2/6)			++(5/5)	++(7/7)	++(6/6)
ZG *S_3S_5*									--(2/2)						
SJ *S_5S_6*	++(8/8)			++(7/7)		+(2/4) ++(2/4)	+(3/5) ++(2/5)			--(5/5)				++(6/6)	++(7/7)
HB *S_2S_7*	+(3/3)	++(8/8)		+(5/5)		+(4/4)	++(5/5)	++(1/1)		++(5/5)	--(8/8)		++(5/5)	+(3/4) ++(1/4)	++(4/4)
CL *S_1S_7*												-- (5/5)			
HN *S_1S_8*	+(4/6) ++(2/6)	+(4/7) ++(3/7)		++(7/7)		++(3/3)	++(5/5)	++(6/6)		++(6/6)			--(13/13)	+(5/8) ++(3/8)	+(5/7) ++(2/7)
SU *S_2S_8*	+(2/2)					+(2/2)	++(4/4)			++(3/3)	+(4/4)			--(2/2)	+(3/3)
GX *S_8S_9*	++(4/4)			++(9/9)		++(8/8)	++(7/7)			++(8/8)				+(2/4) ++(2/4)	--(6/6)

Supplementary Table 5. Compatibility relationships between different pummelo accessions, as assigned by aniline blue staining.

The classification of pollinations to incompatible ("--"), half-compatible ("+") and fully compatible ("++") was performed by assessing aniline blue staining of pistils after pollination using multiple pollinations (see **Supplementary Fig. 7**). This method was used to assign the *S*-genotype of the pummelo accessions. For clarity and to show confidence in the assignment of these classifications, we have indicated the raw data here, showing the number of aniline blue pistils assigned to a particular compatibility class out of the number of pollinations made (indicated in the brackets; e.g. 5/5 indicates 5 classifications assigned this class out of 5 pollinations). We have also indicated the misclassifications here (indicated by red font), to show how we built confidence for the half-compatible assignments (e.g. 1/5 indicates 1 classification assigned this class out of 5 pollinations). Performing multiple pollinations and assigning classifications in a block like this allows us to cross-check predicted outcomes and helps lend confidence to the classifications assigned. Here we show the result of 583 pollinations, of which 44 (< 8%) were misclassified; in all cases, it was clear what the correct classification should be, because of the pattern in which the pollinations were made.

The assignment of these classification classes (see **Supplementary Fig. 7** for examples of the pollinations) was as follows: When almost all pollen tubes were inhibited near the top of the style, the cross was assigned as fully-incompatible ("--", indicated by yellow boxes), with the same two *S*-alleles shared between the parents. When many pollen tube bunches extended to the base of the pistil, the cross was assigned as fully-compatible ("++", indicated by blue boxes), confirming that the parents did not share either *S*-alleles. When pollinations showed some pollen tubes inhibited in the upper style but some extended through the pistil, the cross was assigned as half-compatible ("+", indicated by green boxes), indicating that the parents have one common *S*-allele between them.

The numbering of *S*-alleles was started at S_1S_2 for the first plant genotype. Compatibility with subsequent plants determined the assigned numbers: completely new numbers if assigned as fully compatible (as they cannot share any *S*-alleles), one new number if assigned as half-compatible (as they must share one *S*-allele), and the same number if assigned as incompatible (as they must share both *S*-alleles). In this way the accessions previously assigned the two-letter code (e.g. ST) were assigned an *S*-genotype.

Supplementary Table 6. List of primer sequences

Name	Primer	Target / Purpose
F-R1-F	ATGAACATTACTTTCTTCCTCTA	Full-length amplification of *S1-RNase*
F-R1-R	TTAAGGCGGGGGAAAGGTA	
F-R2-F	ATGATATCGACAAAGACGAAAA	Full-length amplification of *S2-RNase*
F-R2-R	CTACTCATCGGTCGGCTCG	
F-R3-F	ATGAAGACGAAGGCAACTTAC	Full-length amplification of *S3-RNase*
F-R3-R	CTACTTAGTCGGACTCGGAGCAG	
F-R4-F	ATGAGTGCTACTCTCTTCATTTTC	Full-length amplification of *S4-RNase*
F-R4-R	TTATTTAGGCGGGGGAAAG	
F-R5-F	ATGAAGGTGGCATCCATCAAC	Full-length amplification of *S5-RNase*
F-R5-R	CTACCACCGTGGTGGGAAAATAATATCC	
F-R6-F	ATGGGGACTAATTTCCTCATTATC	Full-length amplification of *S6-RNase*
F-R6-R	CTATATTTTAACGTATCGCGGC	
F-R7-F	ATGAAGGCAGCTTATCTTCTTTC	Full-length amplification of *S7-RNase*
F-R7-R	TCAGGAGCTGCTAATTTGAACCTTGG	
F-R8-F	ATGGGGATTGGTTTCCTCATTTTC	Full-length amplification of *S8-RNase*
F-R8-R	TTATTCTTCATGCCAAATATATCCATTCTC	
F-R9-F	ATGAAGACAAGGGCAACTTAC	Full-length amplification of *S9-RNase*
F-R9-R	CTACTTAGTCCGAGTAGGGAAC	
F-Rm-F	ATGAAGATTAATTTCTGCATTTTC	Full-length amplification of *Sm-RNase*
F-Rm-R	TTATTTATGCCGGGGGGAAGCTGATAAC	
S-R1-F	ATGAACATTACTTTCTTCCTCTACA	Specific amplification of *S1-RNase*
S-R1-R	GTTGATCTCCGTTCTTCGTG	
S-R2-F	GACTAACCTCTTTCGCTTTGC	Specific amplification of *S2-RNase*
S-R2-R	CGGATCCATGCCTTTTCTAG	
S-R3-F	TCCAACATCACCTATTGTACAGC	Specific amplification of *S3-RNase*
S-R3-R	GATAACGACCATCACTAAAAACG	
S-R4-F	GTTTGTTTCCTGCATTTCCTC	Specific amplification of *S4-RNase*
S-R4-R	GACCCCTGTTCTTTTTTACTGC	
S-R5-F	ATGAAGGTGGCATCCATCA	Specific amplification of *S5-RNase*
S-R5-R	AATAATATCCGGCCCACAG	
S-R6-F	ATGGGGACTAATTTCCTCATTATCTTT	Specific amplification of *S6-RNase*
S-R6-R	CTATATTTTAACGTATCGCGGCAA	
S-R7-F	TCTTTCTTTTGTTTTGCTTGTTC	Specific amplification of *S7-RNase*
S-R7-R	ATTTGAACCTTGGAAGGGAAC	
S-R8-F	GTTGTAACGCAAAACACTTCTG	Specific amplification of *S8-RNase*
S-R8-R	CGTATGAGCATGTTAGTCTTGG	
S-R9-F	CATTACCTATTCTGCTGCTCA	Specific amplification of *S9-RNase*
S-R9-R	CCGAGTAGGGAACATGATTG	
q-R1-F	AAGGCCATCAGATTTCGTTC	qRT-PCR of *S1-RNase*
q-R1-R	CAGTGCTCATCCATTTCCATAC	
q-R2-F	TTCATCCTACATGGGCTCTG	qRT-PCR of *S2-RNase*
q-R2-R	TATCTCGCTTCAGCGATTTTAG	
q-R3-F	CCAACATCACCTATTGTACAGC	qRT-PCR of *S3-RNase*
q-R3-R	ACGAACCATGTTACATTACGG	

q-R4-F	GTGCTACTCTCTTCATTTTCATTG	qRT-PCR of *S_4-RNase*
q-R4-R	CTGATGCTTTTCTTTTACAGTTG	
q-R5-F	GCATCCATCAACATCTGTATTC	qRT-PCR of *S_5-RNase*
q-R5-R	TGAAGAACGAAGACTCCTGG	
q-R6-F	GCAAAATCCCTGCAATAACC	qRT-PCR of *S_6-RNase*
q-R6-R	CTGGAAATTCTTGAATGTGTGG	
q-R7-F	CCGCAATGGAACAAGTCTAC	qRT-PCR of *S_7-RNase*
q-R7-R	GCCAGTATTTTCCCATATCACTC	
q-R8-F	GGTTGTAACGCAAAACACTTC	qRT-PCR of *S_8-RNase*
q-R8-R	AGGGGTATTTCTGGCAGAAG	
q-R9-F	GCATTACCTATTCTGCTGCTC	qRT-PCR of *S_9-RNase*
q-R9-R	TGACGAACCTTGATACATTTCG	
q-Actin-F	ATCTGCTGGAAGGTGCTGAG	qRT-PCR of *Actin*
q-Actin-R	CCAAGCAGCATGAAGATCAA	
A-R2-F	TTCATCCTACATGGGCTCTG	Absolute quantification of *S_2-RNase*
A-R2-R	TATCTCGCTTCAGCGATTTTAG	
A-Rm-F	AGGACGAGATCCGTACAAACATA	Absolute quantification of *S_m-RNase*
A-Rm-R	GTTTCCCAGTAACTCCTTCCATC	
RT-R2-F	GACTAACCTCTTTCGCTTTGC	RT-PCR of *S_2-RNase*
RT-R2-R	CGGATCCATGCCTTTTCTAG	
RT-Rm-F	AACAGATTTCGTCCTACACGG	RT-PCR of *S_m-RNase*
RT-Rm-R	CCAAAAGAATGATTGCGTAGC	
F-F1-1-F	ATGGTGATGACAAGCTATGGAG	Full-length amplification of *S_1-SLF1*
F-F1-1-R	CTATATATCCTCTTCTCTTACTATAATTAGAC	
F-F1-2-F	ATGACGGTGATGACAGGC	Full-length amplification of *S_1-SLF2*
F-F1-2-R	TCAGAGTGTAATCAGACTCTCT	
F-F1-3-F	ATGGGGAGAGAGACGACG	Full-length amplification of *S_1-SLF3*
F-F1-3-R	TTATGTATCCTCTTCTCTAACTATAATTAG	
F-F1-4-F	ATGGCGAGAGAGGCTAGGGT	Full-length amplification of *S_1-SLF4*
F-F1-4-R	CTACATATCCTCTTCCTTCACTCTAAT	
F-F1-5-F	ATGATGGTGACCTGTACTGG	Full-length amplification of *S_1-SLF5*
F-F1-5-R	TTATAAATACACACCCAATGTATG	
F-F1-6-F	ATGGTAGAAAGCAATGGAGA	Full-length amplification of *S_1-SLF6*
F-F1-6-R	TTATTCCACTCCTAAGATATGCCATGG	
F-F1-7-F	ATGGTGTTATTTGGCAAAGACG	Full-length amplification of *S_1-SLF7*
F-F1-7-R	TCAAACTCCTTCTGTTTGATACACAC	
F-F1-8-F	ATGGCGAAATGTAACGGA	Full-length amplification of *S_1-SLF8*
F-F1-8-R	TTAACAGGAATTAGTTTGATAAACC	
F-F1-9-F	ATGATGACAAGTGATGAACAG	Full-length amplification of *S_1-SLF9*
F-F1-9-R	CTATGGGAGTGATGCATCGATTAG	
F-F2-1-F	ATGGTGATGACAAGCTATGGAG	Full-length amplification of *S_2-SLF1*
F-F2-1-R	CTAAATATCTTCTTTTCTGACAATAATTAG	
F-F2-2-F	ATGGAGAGAGATATGTCGGTGAT	Full-length amplification of *S_2-SLF2*
F-F2-2-R	CTATTCTTGGATTTTAATTAGACTTTCC	
F-F2-3-F	ATGGAGAGGGAGATGATGG	Full-length amplification of *S_2-SLF3*
F-F2-3-R	CTATATATCCTCTACTCTAACTGAAATTAGAC	
F-F2-4-F	ATGGCCAGAGAGACAAGG	Full-length amplification of *S_2-*

F-F2-4-R	TTACTTCATTCTAATTAAACTCTCTTTTAAAATATG	*SLF4*
F-F2-5-F	ATGGTGATAAATACTGGAGACTT	Full-length amplification of *S*$_2$-*SLF5*
F-F2-5-R	TTAATACACACCCAATGTATGC	
F-F2-6-F	ATGGCGATAATGGTGGAAAGC	Full-length amplification of *S*$_2$-*SLF6*
F-F2-6-R	TCATTCATGTTCCACACCTAAGATATG	
F-F2-7-F	ATGGTGTTATTAGACAACGAAGATTCAT	Full-length amplification of *S*$_2$-*SLF7*
F-F2-7-R	TCATTCTGTTTGATTTACATCCAAAAC	
F-F2-8-F	ATGGCGAAAAGCAACAGCAAGT	Full-length amplification of *S*$_2$-*SLF8*
F-F2-8-R	TTAACAGGAATTAGTTTGATAAACTCCCA	
F-F2-9-F	ATGATGATGACAAGTAATGAAG	Full-length amplification of *S*$_2$-*SLF9*
F-F2-9-R	CTAGGGGAGAGATCCATCATCG	
S-F1-1-F	GGTTGAGACACTATCGAGGTTG	Specific amplification of *S*$_1$-*SLF1*
S-F1-1-R	CTTTCCTCATCGACTAAGGTG	
S-F1-2-F	TTATTGGGTGGCATCGGG	Specific amplification of *S*$_1$-*SLF2*
S-F1-2-R	CATAAACCGGTAATTCCAAGATCC	
S-F1-3-F	TGAATACAGAGTTGTTCCAGG	Specific amplification of *S*$_1$-*SLF3*
S-F1-3-R	ATGTGCCATCTCTTCTGAATATAG	
S-F1-4-F	CTTCTCTATATTCCCCGATAAGAC	Specific amplification of *S*$_1$-*SLF4*
S-F1-4-R	AGAATGTGCGAACTTATCCG	
S-F1-5-F	TGCAACTAAGGAGTCTAGGGC	Specific amplification of *S*$_1$-*SLF5*
S-F1-5-R	TTAAAGTCTCCGTATAGTTGCG	
S-F1-6-F	TGAATACAGAGTTGTTCCAGG	Specific amplification of *S*$_1$-*SLF6*
S-F1-6-R	ATGTGCCATCTCTTCTGAATATAG	
S-F1-7-F	AATACACGAGGGTTTTTGGTAC	Specific amplification of *S*$_1$-*SLF7*
S-F1-7-R	CCCGGTATCAGGCTCATAC	
S-F1-8-F	TGGCGAAATGTAACGGAAAT	Specific amplification of *S*$_1$-*SLF8*
S-F1-8-R	CAAATCCCATAATAGTATCA	
S-F1-9-F	GATGGAGCGTTTGATAGCG	Specific amplification of *S*$_1$-*SLF9*
S-F1-9-R	CCTCTTTCTTCACTCCAATAAGAC	
S-F2-1-F	CCACGTAATACGACGGCTAAC	Specific amplification of *S*$_2$-*SLF1*
S-F2-1-R	GAAAGGTCCGAAGGTCAAG	
S-F2-2-F	GGTGATGACACGCTGTGAAG	Specific amplification of *S*$_2$-*SLF2*
S-F2-2-R	AAGTATTGCTGGGAAGACGAG	
S-F2-3-F	CAATGAGGGGAACTACAACTGG	Specific amplification of *S*$_2$-*SLF3*
S-F2-3-R	GTATCCAAGGACTCATCGCTG	
S-F2-4-F	TATTCCCTGATAGGACACTAACAG	Specific amplification of *S*$_2$-*SLF4*
S-F2-4-R	CCCAGTAACAATATCCATTCAAG	
S-F2-5-F	AACTAAAGAGTATAGACCTGTCCC	Specific amplification of *S*$_2$-*SLF5*
S-F2-5-R	CAAGTGGCTTAGACACTCCTA	
S-F2-6-F	CTCACCTTGTTGGATACGAAAATAG	Specific amplification of *S*$_2$-*SLF6*
S-F2-6-R	ACATAAAACCACAAACCTCGTAGC	
S-F2-7-F	TGGTTGAAATTCTATCCAGGCTAC	Specific amplification of *S*$_2$-*SLF7*
S-F2-7-R	ATATTTCGGGAGAGTAATGGACTC	
S-F2-8-F	TGCCGGAGGATGTTATTATTG	Specific amplification of *S*$_2$-*SLF8*
S-F2-8-R	GAAGAGTTCTTGACTCCTTGGTTG	
S-F2-9-F	GGAGAAGCACGACGGACCTGA	Specific amplification of *S*$_2$-*SLF9*
S-F2-9-R	CGTTACCTAGATGAAACGAAAGAAT	

q-F1-1-F	ACTTTACTCAGAAGACGTCGC	qRT-PCR of *S₁-SLF1*
q-F1-1-R	CAGTCGTTTGTCATTTGATTCT	
q-F1-2-F	GTCATTCAGCATGAGTGACGAG	qRT-PCR of *S₁-SLF2*
q-F1-2-R	CAACCATCGTATATGCCTATCG	
q-F1-3-F	GTACGCCGTCCTGATTATTAC	qRT-PCR of *S₁-SLF3*
q-F1-3-R	CATCCAAGGTCTCATCGC	
q-F1-4-F	CAGTCAGTGAAGACACCTTGG	qRT-PCR of *S₁-SLF4*
q-F1-4-R	AGAATGTGCGAACTTATCCG	
q-F1-5-F	GAGACTCACTCCGATCAGATG	qRT-PCR of *S₁-SLF5*
q-F1-5-R	TTAAAGTCTCCGTATAGTTGCG	
q-F1-6-F	GAAATGTTGTTACGATTGCCG	qRT-PCR of *S₁-SLF6*
q-F1-6-R	ACAGTATACCAAGAGACGGGTGT	
q-F1-7-F	CCAACCACTCCTGTTTTGG	qRT-PCR of *S₁-SLF7*
q-F1-7-R	CCCGGTATCAGGCTCATAC	
q-F1-8-F	GGATTTGGATTGGATATTATGAG	qRT-PCR of *S₁-SLF8*
q-F1-8-R	GGATTTGGATTGGATATTATGAG	
q-F1-9-F	GGGGTTTGTTATTGGTTATCT	qRT-PCR of *S₁-SLF9*
q-F1-9-R	TATGGCTCCTGTATTTCTTCG	
q-F2-1-F	TGCCTTTCTTTGCTATACTCAG	qRT-PCR of *S₂-SLF1*
q-F2-1-R	GAAAGGTCCGAAGGTCAAG	
q-F2-2-F	ACTTGGTCCTTGTGATGGTAT	qRT-PCR of *S₂-SLF2*
q-F2-2-R	AAGTATTGCTGGGAAGACGAG	
q-F2-3-F	CAATGAGGGGAACTACAACTG	qRT-PCR of *S₂-SLF3*
q-F2-3-R	GAAGGCGAACTTCATAGCC	
q-F2-4-F	GTTGCATTGGGTTTAGATCTC	qRT-PCR of *S₂-SLF4*
q-F2-4-R	CATGAAACGAATCTCTTTGATC	
q-F2-5-F	AGTAAATGCGGTGATGGG	qRT-PCR of *S₂-SLF5*
q-F2-5-R	GTCTTTAATCGTCCATATTTCC	
q-F2-6-F	GGATTATTCGATGACTTACTGTCTC	qRT-PCR of *S₂-SLF6*
q-F2-6-R	GTGTCAGGATCGTATAAGAGTAGTTG	
q-F2-7-F	TGAATCTAACTCTTCACAGTTGCTC	qRT-PCR of *S₂-SLF7*
q-F2-7-R	AAACCAACAGCATTCGAGTTC	
q-F2-8-F	TGCCGGAGGATGTTATTATTG	qRT-PCR of *S₂-SLF8*
q-F2-8-R	CTCTGCATACACACCTGAATCTTAG	
q-F2-9-F	CGCTACGTGCTAACTCTTGGA	qRT-PCR of *S₂-SLF9*
q-F2-9-R	CAGATAACCAGTAACAAACCC	
BAC-R1-F	TTTATTTCCTGCATTTCCTCGG	Probe used to screen the *S₁*-locus from BAC library
BAC-R1-R	ACTCCTTCCATTTGGATATATTCC	
BAC-R1-5'-F	GGAACCAAGACCAAGTACCATTATG	
BAC-R1-5'-R	AGTAAGAACTGACCAAAATTCACAG	
BAC-R1-3'-F	GAATCATCGTTTTGTGAAGAAGAG	
BAC-R1-3'-R	TCAATGCGGAGTTTAGGAAGA	
BAC-R2-F	CTCTTGAGGCTGATTTGATG	Probe used to screen the *S₂*-locus from BAC library
BAC-R2-R	CGGGGAACTTGATATTGTCT	
BAC-R2-5'-F	ACAAAACGCCATATAGAAAGAGTC	
BAC-R2-5'-R	CATCCAAAGGAGTAATTCATCAC	
6P-R1-F	CGGAATTCAACAATTCTGGTTTTGACCACTT	*S₁-RNase* cloned to pGEX-6P-1

6P-R1-R	CCCTCGAGTTAAGGCGGGGGAAAGGTA	
6P-R2-F	CGGAATTCTCCTCGCAATTGTTCGACC	*S₂-RNase* cloned to pGEX-6P-1
6P-R2-R	CCCTCGAGCTACTCATCGGTCGGCTCG	
6P-Rm-F	GGATCCCCGGAATTCAATTCTGGTTTTGACCACTTTTGGC	*Sm*-RNase cloned to pGEX-6P-1
6P-Rm-R	ATGCGGCCGCTCGAGTTATTTATGCCGGGGGAAGCTGATAAC	
6P-Rm^R-F	GGATCCCCGGAATTCAATTCTGGTTTTGACCACTTTTGGC	*Sm^R*-RNase cloned to pGEX-6P-1
6P-Rm^R-overlap-R	GATTTCTTAGTATTCTCAGCAGGTTCACAC	
6P-Rm^R-overlap-F	GAATACTAAGAAATCAAGGAATATTTCCAGATGG	
6P-Rm^R-R	ATGCGGCCGCTCGAGTTATTTATGCCGGGGGAAGCTGATAAC	

Allele-specific primers were used to amplify full-length *S-RNases*; forward (F) and reverse (R).

Supplementary Table 7. Information regarding the BAC clones for the pummelo *S*$_1$- and *S*$_2$-loci

Locus	Clone	Number of read pairs	Clean bases (G)	Read length (bp)	GC (%)	SRR id in GenBank
S$_1$-locus	84-N-5	4720	1.42	150	35.8	SRR10168706
	10-J-4	4450	1.34	150	39.07	SRR10168705
	51-O-18	4597	1.38	150	39.96	SRR10168704
S$_2$-locus	72-E-8	3803	1.14	150	35.04	SRR10168708
	57-F-22	4607	1.38	150	43.34	SRR10168709

A BAC library constructed from a pummelo of genotype *S*$_1$*S*$_2$ was arrayed in 108 different 384-well microtiter plates. Clones (three for the *S*$_1$-locus and two for the *S*$_2$-locus) were screened by using the probes (**Supplementary Table 6**) of *S*$_1$-*RNase* and *S*$_2$-*RNase* respectively. Clones were identified as containing the *S*-locus by sequencing, using the Illumina platform.

Supplementary Table 8. Other genes identified at the *S*$_1$-locus with functions predicted by the Swissprot database.

Gene	Annotation	E value	Description
S1.gene1	Transformation/transcription domain-associated protein	0	
S1.gene2	Unknown		
S1.gene3	Unknown		
S1.gene4	Cytokinin riboside 5'-monophosphate phosphoribohydrolase	4.77E-101	
S1.gene5	Unknown		
S1.gene6	Unknown		
S1.gene7	Unknown		
S1.gene8	Putative AC transposase	1.44E-91	
S1.gene9	Unknown		
S1.gene10	Retrovirus-related Pol polyprotein from transposon	6.33E-14	
S1.gene11	Unknown		
S1.gene12	Putative ribonuclease H protein	9.48E-21	
S1.gene13	**F-box/kelch-repeat protein**	**1.58E-19**	***S*$_1$*-SLF2***
S1.gene14	Unknown		
S1.gene15	Retrovirus-related Pol polyprotein from transposon	2.02E-55	
S1.gene16	Unknown		
S1.gene17	Unknown		
S1.gene18	CENP-B homolog protein 2	7.35E-55	
S1.gene19	Unknown		
S1.gene20	Unknown		
S1.gene21	**Putative F-box protein**	**2.22E-18**	***S*$_1$*-SLF1***
S1.gene22	Unknown		
S1.gene23	Unknown		
S1.gene24	Unknown		
S1.gene25	Unknown		
S1.gene26	Unknown		
S1.gene27	Retrovirus-related Pol polyprotein from transposon	8.88E-05	
S1.gene28	Retrovirus-related Pol polyprotein from transposon	1.97E-07	
S1.gene29	**Nicotiana alata Ribonuclease S7**	**5.99E-28**	***S*$_1$*-RNase***
S1.gene30	Probable cytokinin riboside 5'-monophosphate phosphoribohydrolase	1.77E-10	
S1.gene31	Copia protein	3.85E-10	
S1.gene32	Unknown		
S1.gene33	Unknown		
S1.gene34	**F-box/kelch-repeat protein**	**5.07E-23**	***S*$_1$*-SLF6***
S1.gene35	Unknown		
S1.gene36	Unknown		

S1.gene37	**Putative F-box protein**	**5.32E-15**	***S1-SLF5***
S1.gene38	Unknown		
S1.gene39	Cytochrome P450	2.52E-132	
S1.gene40	Unknown		
S1.gene41	**F-box protein**	**4.58E-17**	***S1-SLF4***
S1.gene42	Retrovirus-related Pol polyprotein from transposon opus	8.99E-06	
S1.gene43	Pol polyprotein (Fragment)	5.89E-12	
S1.gene44	Probable cytokinin riboside 5'-monophosphate phosphoribohydrolase	1.49E-12	
S1.gene45	Unknown		
S1.gene46	Unknown		
S1.gene47	Unknown		
S1.gene48	**Putative F-box protein**	**1.13E-17**	***S1-SLF3***
S1.gene49	Unknown		
S1.gene50	**F-box protein CPR1**	**1.32E-17**	***S1-SLF7***
S1.gene51	**F-box/kelch-repeat protein**	**7.49E-21**	***S1-SLF9***
S1.gene52	**F-box/kelch-repeat protein**	**3.00E-18**	***S1-SLF8***
S1.gene53	Protein indeterminate-domain 7	1.95E-49	
S1.gene54	Calcium-dependent protein kinase 16	0	
S1.gene55	Unknown		
S1.gene56	DNA-(apurinic or apyrimidinic site) lyase 2	0	
S1.gene57	Unknown		
S1.gene58	**Putative F-box/kelch-repeat protein**	**9.04E-14**	***S1-SLFL10***
S1.gene59	**Putative F-box/kelch-repeat protein**	**1.32E-15**	***S1-SLFL11***
S1.gene60	Unknown		
S1.gene61	**F-box protein**	**1.18E-18**	***S1-SLFL12***

Supplementary Table 9. Other genes identified at the *S*$_2$-locus with functions predicted by the Swissprot database.

Gene	Annotation	E value	Description
S2.gene1	Transcription-associated protein	0	
S2.gene2	Unknown		
S2.gene3	Unknown		
S2.gene4	Cytokinin riboside 5'-monophosphate phosphoribohydrolase	1.37E-101	
S2.gene5	**Putative F-box protein**	**2.72E-22**	***S*$_2$*-SLF1***
S2.gene6	Unknown		
S2.gene7	Unknown		
S2.gene8	Unknown		
S2.gene9	**F-box/kelch-repeat protein**	**4.21E-18**	***S*$_2$*-SLF2***
S2.gene10	Unknown		
S2.gene11	Unknown		
S2.gene12	**F-box protein**	**2.46E-16**	***S*$_2$*-SLF3***
S2.gene13	Unknown		
S2.gene14	Retrovirus-related Pol polyprotein from transposon	1.43E-37	
S2.gene15	**Putative F-box protein**	**1.63E-15**	***S*$_2$*-SLF4***
S2.gene16	Unknown		
S2.gene17	L10-interacting MYB domain-containing protein	1.18E-06	
S2.gene18	Unknown		
S2.gene19	Unknown		
S2.gene20	**F-box protein**	**7.54E-16**	***S*$_2$*-SLF5***
S2.gene21	Retrovirus-related Pol polyprotein from transposon	2.62E-13	
S2.gene22	Retrovirus-related Pol polyprotein from transposon	1.46E-45	
S2.gene23	Retrovirus-related Pol polyprotein from transposon	1.20E-31	
S2.gene24	Retrovirus-related Pol polyprotein from transposon	2.25E-24	
S2.gene25	Unknown		
S2.gene26	Unknown		
S2.gene27	Unknown		
S2.gene28	**Petunia hybrida Ribonuclease S3**	**8.86E-17**	***S*$_2$*-RNase***
S2.gene29	Retrovirus-related Pol polyprotein from transposon	5.06E-169	
S2.gene30	Spermidine synthase 2	1.21E-06	
S2.gene31	Unknown		
S2.gene32	Unknown		
S2.gene33	Unknown		
S2.gene34	**F-box/kelch-repeat protein**	**9.07E-22**	***S*$_2$*-SLF6***
S2.gene35	**F-box/kelch-repeat protein**	**1.55E-16**	***S*$_2$*-SLF7***
S2.gene36	Unknown		

S2.gene37	Unknown		
S2.gene38	Unknown		
S2.gene39	Unknown		
S2.gene40	**F-box/kelch-repeat protein**	**9.15E-17**	***S_2-SLF9***
S2.gene41	**F-box/kelch-repeat protein**	**1.16E-20**	***S_2-SLF8***
S2.gene42	Calcium-dependent protein kinase 16	0	
S2.gene43	Unknown		
S2.gene44	DNA-(apurinic or apyrimidinic site) lyase 2	0	
S2.gene45	Unknown		
S2.gene46	**Putative F-box protein**	**2.33E-14**	***S_2-SLFL10***
S2.gene47	**Putative F-box/kelch-repeat protein**	**2.51E-16**	***S_2-SLFL11***
S2.gene48	Unknown		
S2.gene49	**F-box protein**	**2.97E-19**	***S_2-SLFL12***
S2.gene50	ABC transporter G family member 36	1.66E-27	
S2.gene51	ABC transporter G family member 40	4.34E-120	

Supplementary Table 10. Pairwise sequence identities of the deduced amino acid sequence between the citrus Type 1 to Type 12 SLFs/SLFLs

Type 1	Predicted interaction: S_1-RNase + S_2/S_6/S_{10}/S_{11}/S_{12}/S_{13}/S_{14}-SLF1						
	S_2-SLF1	S_6-SLF1	S_{10}-SLF1	S_{11}-SLF1	S_{12}-SLF1	S_{13}-SLF1	S_{14}-SLF1
S_1-SLF1	89.646	88.011	87.466	88.011	88.767	88.556	88.011
S_2-SLF1		97.82	97.548	97.275	98.356	98.365	97.82
S_6-SLF1			97.275	97.275	97.275	97.82	97.275
S_{10}-SLF1				98.365	97.275	97.275	97.275
S_{11}-SLF1					97.275	97.275	97.275
S_{12}-SLF1						97.82	97.82
S_{13}-SLF1							97.82

90%＜Identity
80%＜Identity≤90%
70%＜Identity≤80%
Identity≤70%

Type 2	Predicted interaction: S_2-RNase + S_1/S_{11}/S_m/S_{13}/S_{10}/S_6/S_{12}/S_{14}-SLF2							
	S_1-SLF2	S_{11}-SLF2	S_m-SLF2	S_{13}-SLF2	S_{10}-SLF2	S_6-SLF2	S_{12}-SLF2	S_{14}-SLF2
S_2-SLF2	78.082	79.784	80.165	75.202	79.515	80.863	80.054	80.495
S_1-SLF2		87.123	87.637	78.356	82.74	84.384	83.836	84.254
S_{11}-SLF2			89.286	82.933	86.933	88.533	87.733	86.685
S_m-SLF2				80.939	86.188	86.813	85.635	86.188
S_{13}-SLF2					86.667	90.667	85.867	85.87
S_{10}-SLF2						93.867	92	91.848
S_6-SLF2							92	92.663
S_{12}-SLF2								90.761

Type3	S_2-SLF3	S_m-SLF3	S_{14}-SLF3	S_{13}-SLF3b	S_6-SLF3	S_{10}-SLF3	S_{12}-SLF3	S_{13}-SLF3a	S_{11}-SLF3
S_1-SLF3	85.561	87.838	86.957	88.525	87.601	87.062	87.433	87.968	88.41
S_2-SLF3		88.076	86.413	86.649	85.714	86.096	85.829	86.631	88.076
S_m-SLF3			85.87	88.556	87.297	88.076	87.568	88.108	88.618
S_{14}-SLF3				88.011	86.957	87.772	88.043	88.587	90.217
S_{13}-SLF3b					89.101	89.373	89.101	90.191	89.918
S_6-SLF3						92.992	90.836	94.879	90.323
S_{10}-SLF3							90.909	94.609	90.786
S_{12}-SLF3								93.048	90.296
S_{13}-SLF3a									91.87

Type 4	Predicted interaction: S_6-RNase + S_m/S_{10}/S_{11}/S_1/S_2/S_{12}/S_{14}/S_{13}-SLF4							
	S_m-SLF4	S_{10}-SLF4	S_{11}-SLF4	S_1-SLF4	S_2-SLF4	S_{12}-SLF4	S_{14}-SLF4	S_{13}-SLF4
S_6-SLF4	75.946	77.717	76.902	77.151	78.202	77.957	76.075	77.628
S_m-SLF4		86.141	84.511	87.568	86.649	87.297	86.757	88.076
S_{10}-SLF4			88.889	87.772	87.738	89.946	88.859	89.946
S_{11}-SLF4				88.043	87.193	89.13	88.043	89.402
S_1-SLF4					89.373	88.71	88.172	90.786
S_2-SLF4						89.101	90.463	92.371
S_{12}-SLF4							88.71	90.217
S_{14}-SLF4								91.328

Type 5	Predicted interaction: S_{13}-RNase + S_{14}/S_{12}/S_1/ S_2/S_6/S_{10}/S_{11}/S_m-SLF5							
	S_{14}-SLF5	S_{12}-SLF5	S_1-SLF5	S_2-SLF5	S_6-SLF5	S_{10}-SLF5	S_{11}-SLF5	S_m-SLF5
S_{13}-SLF5	46.518	46.089	47.765	45.81	48.324	47.887	47.632	49.162
S_{14}-SLF5		73.925	77.688	75.806	75.806	76.216	76.882	77.419
S_{12}-SLF5			82.62	81.867	82.842	86.933	80	82.667
S_1-SLF5				84.225	85.791	85.294	82.62	85.294
S_2-SLF5					86.327	85.6	83.2	86.4
S_6-SLF5						86.863	83.646	87.131
S_{10}-SLF5							82.4	86.4
S_{11}-SLF5								83.2

Type 6	S_m-SLF6	S_{12}-SLF6	S_{10}-SLF6	S_6-SLF6	S_{11}-SLF6	S_1-SLF6	S_2-SLF6	S_{13}-SLF6a	S_{14}-SLF6
S_{13}-SLF6b	57.796	56.72	56.989	56.452	57.796	58.333	58.333	58.491	58.602
S_m-SLF6		87.366	87.903	88.889	88.71	89.008	88.472	88.978	88.889
S_{12}-SLF6			90.667	89.067	89.572	89.247	87.733	87.968	88
S_{10}-SLF6				89.6	87.433	89.247	87.733	88.235	87.733
S_6-SLF6					87.701	90.323	88.564	89.572	88.451
S_{11}-SLF6						90.054	89.037	89.182	88.503
S_1-SLF6							89.247	90.323	89.516
S_2-SLF6								90.909	90.133
S_{13}-SLF6a									90.909

Type 7		Predicted interaction: S_{10}/S_{12}-RNase + S_{11}/S_2/S_1/S_{13}/S_{14}/S_m-SLF7 and S_6-SLF7a/b							
	S_{12}-SLF7	S_{11}-SLF7	S_2-SLF7	S_1-SLF7	S_6-SLF7a	S_6-SLF7b	S_{13}-SLF7	S_{14}-SLF7	S_m-SLF7
S_{10}-SLF7	84.777	80.366	80.628	81.365	82.275	83.508	83.508	81.675	82.723
S_{12}-SLF7		80.628	81.414	81.89	82.54	83.246	83.77	82.461	82.723
S$_{11}$-SLF7			85.676	86.702	86.863	85.942	86.207	86.737	85.942
S_2-SLF7				88.298	90.323	88.859	89.39	89.125	89.655
S_1-SLF7					91.421	92.021	92.287	90.691	92.287
S_6-SLF7a						91.153	91.421	92.493	91.957
S_6-SLF7b							98.939	90.981	92.838
S_{13}-SLF7								91.247	93.103
S_{14}-SLF7									92.042

Type 8	S_{12}-SLF8a	S_2-SLF8	S_6-SLF8b	S_{12}-SLF8b	S_{11}-SLF8	S_1-SLF8	S_6-SLF8a	S_{10}-SLF8b	S_{13}-SLF8a	S_{13}-SLF8b	S_{14}-SLF8	S_m-SLF8
S_{10}-SLF8a	87.566	83.158	80.576	80.789	82.895	82.632	83.158	82.895	79.211	81.053	83.158	83.158
S_{12}-SLF8a		83.069	80.216	82.275	83.069	83.069	84.392	83.333	79.894	80.952	83.598	83.598
S_2-SLF8			89.928	88.158	92.895	93.684	92.105	93.947	88.421	89.211	92.895	92.368
S_6-SLF8b				89.209	90.288	92.806	93.165	94.245	88.489	89.568	94.245	93.165
S_{12}-SLF8b					88.684	90.526	90.789	90.789	86.579	88.158	91.053	90.789
S_{11}-SLF8						93.947	92.632	94.211	88.158	88.947	92.895	92.632
S_1-SLF8							96.579	98.158	92.105	92.895	96.579	96.842
S_6-SLF8a								96.842	92.895	93.421	96.579	96.579
S_{10}-SLF8b									92.895	93.684	97.105	97.632
S_{13}-SLF8a										92.105	92.632	92.632
S_{13}-SLF8b											93.421	93.421
S_{14}-SLF8												97.105

Type 9	Predicted interaction: S_{11}/S_{13}/S_{14}-RNase + S_2/S_{12}/S_1/S_{10}/S_m-SLF9 and S_6-SLF9a/b					
	S_2-SLF9	S_{12}-SLF9	S_1-SLF9	S_6-SLF9a	S_{10}-SLF9	S_m-SLF9
S_{11}/S_{13}/S_{14}-SLF9 are absent						
S_6-SLF9b	86.942	86.598	88.66	87.973	88.66	88.66
S_2-SLF9		87.139	86.877	86.387	87.5	87.5
S_{12}-SLF9			90.263	90	90	90
S_1-SLF9				95.263	95.526	95.526
S_6-SLF9a					97.638	97.638
S_{10}-SLF9						100

Type 10	Predicted interaction: S_{13}-RNase + S_{12}/S_1/S_2/S_6/S_{10}/S_{11}/S_m-SLFL10 and S_{14}-SLFL10a/b								
	S_{12}-SLFL10	S_1-SLFL10	S_2-SLFL10	S_6-SLFL10	S_{10}-SLFL10	S_{11}-SLFL10	S_{14}-SLFL10a	S_{14}-SLFL10b	S_m-SLFL10
S_{13}-SLFL10	62.368	68.158	67.895	67.895	68.158	67.368	67.895	67.895	67.632
S_{12}-SLFL10		86.614	86.352	86.614	86.614	85.564	86.352	86.352	86.089
S_1-SLFL10			99.738	99.476	100	98.953	99.738	99.738	99.476
S_2-SLFL10				99.738	99.738	98.691	99.476	99.476	99.215
S_6-SLFL10					99.476	98.429	99.215	99.215	98.953
S_{10}-SLFL10						98.953	99.738	99.738	99.476
S_{11}-SLFL10							98.691	98.691	98.429
S_{14}-SLFL10a								100	99.215
S_{14}-SLFL10b									99.215

Type 11	S_{13}-SLFL11b	S_1-SLFL11	S_2-SLFL11	S_{10}-SLFL11	S_{11}-SLFL11	S_{12}-SLFL11	S_{14}-SLFL11a	S_{14}-SLFL11b	S_m-SLFL11
S_{13}-SLFL11a	89.691	94.33	94.33	93.557	93.668	91.451	93.299	93.299	93.557
S_{13}-SLFL11b		94.898	94.898	94.133	93.963	91.582	93.878	93.878	94.133
S_1-SLFL11			99.49	98.724	98.688	96.173	98.469	98.469	98.724
S_2-SLFL11				98.724	98.688	96.173	98.469	98.469	98.724
S_{10}-SLFL11					98.163	95.408	97.704	97.704	100
S_{11}-SLFL11						95.801	97.638	97.638	98.163
S_{12}-SLFL11							95.153	95.153	95.408
S_{14}-SLFL11a								100	97.704
S_{14}-SLFL11b									97.704

Type 12	S_2-SLFL12	S_6-SLFL12	S_{10}-SLFL12	S_{11}-SLFL12	S_{12}-SLFL12	S_{13}-SLFL12a	S_{13}-SLFL12b	S_{14}-SLFL12a	S_{14}-SLFL12b	S_m-SLFL12
S_1-SLFL12	99.733	99.194	98.663	98.93	97.594	98.396	95.722	98.93	98.93	98.925
S_2-SLFL12		99.462	98.396	98.663	97.326	98.128	95.455	98.663	98.663	98.656
S_6-SLFL12			97.849	98.387	96.774	97.581	94.892	98.118	98.118	98.118
S_{10}-SLFL12				98.663	96.257	97.059	94.652	97.594	97.594	98.118
S_{11}-SLFL12					96.524	97.326	94.652	97.861	97.861	97.849
S_{12}-SLFL12						96.524	94.652	97.059	97.594	96.505
S_{13}-SLFL12a							95.187	97.861	97.861	97.312
S_{13}-SLFL12b								95.455	95.722	94.624
S_{14}-SLFL12a									99.465	97.849
S_{14}-SLFL12b										97.849

These twelve tables show the pairwise % identities (using deduced amino acid sequences) for each of the twelve Types of citrus SLFs (indicated in red font, one for each table) based on pairwise sequence identities

of their deduced amino acid sequences. Different degrees of identity are indicated by grey shading (see key at top). Duplicate SLF copies within each type are indicated by a and b. The predicted interactions between SLF and *S*-RNase (based on the non-self model[8,9,16]) are shown on the top part of each table. The SLFs in each type indicated in orange are either diverged or deleted and their cognate *S*-RNases (also indicated in orange) are predicted to interact with the conserved SLFs under the non-self recognition model.

For type 1 SLFs, the S_1-SLF1 (indicated in orange) sequence is diverged, with 87.5 ~ 89.6% identity with other SLF1s (S_2-, S_6-, S_{10}-, S_{11}-, S_{12}-, S_{13}- and S_{14}-SLF1), while the pairwise identities of the other SLF1s range from 97.3 to 98.4%. The cognate *S*-RNase of S_1-SLF1, S_1-RNase (in orange), is predicted to interact with the S_2-, S_6-, S_{10}-, S_{11}-, S_{12}-, S_{13}- and S_{14}-SLF1 based on the non-self model. Similarly, the S_2-RNase is predicted to interact with the S_1-, S_{11}-, S_m-, S_{13}-, S_{10}-, S_6-, S_{12}- and S_{14}-SLF2 (see type 2 table); the S_6-RNase is predicted to interact with the S_m-, S_{10}-, S_{11}-, S_1-, S_2-, S_{12}-, S_{14}- and S_{13}-SLF4 (see type 4 table); the S_{13}-RNase is predicted to interact with the S_{14}-, S_{12}-, S_1-, S_2-, S_6-, S_{10}- , S_{11}- and S_m-SLF5 (see type 5 table). Both the S_{10}-RNase and S_{12}-RNase are predicted to interact with the S_{11}-, S_2-, S_1-, S_{13}-, S_{14}-, S_m-SLF7 and S_6-SLF7a/b (see type 7 table). The S_{13}-RNase is predicted to interact with the S_{12}-, S_1-, S_2-, S_6-, S_{10}- , S_{11}-, S_m-SLFL10 and S_{14}-SLFL10a/b (see type 10 table). For the type 9 SLFs, the S_{11}-, S_{13}- and S_{14}-SLF9 are deleted. The non-self model predicts that S_{11}-, S_{13}- and S_{14}-RNase could be the target of S_2/S_{12}/S_1/S_{10}/S_m-SLF9 and S_6-SLF9a/b in type 9.

For the type 3, 11 and 12 SLFs, there are no diverged or deleted SLFs and the pairwise SLFs in each type show comparable identities, respectively ranging from 85.6 ~ 94.9%, 89.7 ~ 100%, 94.6 ~ 99.7%. For the type 6, the S_{13}-haplotype has a diverged S_{13}-SLF6b, but it also has a conserved S_{13}-SLF6a. Similarly, the S_{10}-haplotype has a diverged allele (S_{10}-SLF8a) and a conserved allele (S_{10}-SLF8b) in type 8. These suggest that the SLFs in type 3, 6, 8, 11, and 12 do not interact with the *S*-RNases identified in the study.

Supplementary Table 11. Detailed information relating to checking the *S*-haplotypes for 153 *Citrus* accessions

No.	Accession name	Mapped *S*-RNase [a]		Catalog	Scientific name	Source	SRR id
1	DX1	S_m	S_x	Wild mandarin	*C. reticulata*	Wang et al, 2018[17]	SRR5796819
2	DX2	S_m	S_x	Wild mandarin	*C. reticulata*	Wang et al, 2018	SRR5796821
3	DX3	S_m	S_x	Wild mandarin	*C. reticulata*	Wang et al, 2018	SRR5796820
4	DX4	S_m	S_x	Wild mandarin	*C. reticulata*	Wang et al, 2018	SRR5796645
5	MS1	S_m	S_{10}	Wild mandarin	*C. reticulata*	Wang et al, 2018	SRR5796818
6	MS2	S_m	S_{10}	Wild mandarin	*C. reticulata*	Wang et al, 2018	SRR5796635
7	LHJ	S_m	S_x	Wild mandarin	*C. reticulata*	In this study	SRR10163368
8	LRH	S_m	S_x	Wild mandarin	*C. reticulata*	In this study	SRR10163367
9	WLM	S_m	S_{11}	Cultivated mandarin	*C. reticulata*	Wu et al, 2018[18]	SRR1023625
10	ORI	S_m	S_{11}	Cultivated mandarin	*C. reticulata*	Wang et al, 2017[12]	SRR3820595
11	QH117	S_m	S_7	Cultivated mandarin	*C. reticulata*	Wang et al, 2017	SRR3822244
12	18H	S_m	S_7	Cultivated mandarin	*C. reticulata*	Wang et al, 2017	SRR3749605
13	19P	S_m	S_2	Cultivated mandarin	*C. reticulata*	Wang et al, 2017	SRR3747617
14	CSNJ	S_m	S_x	Cultivated mandarin	*C. reticulata*	Wang et al, 2017	SRR3747609
15	CZG	S_m	S_{11}	Cultivated mandarin	*C. reticulata*	Wang et al, 2017	SRR3747583
16	NJ	S_m	S_x	Cultivated mandarin	*C. reticulata*	Wang et al, 2017	SRR3750668
17	HPJ	S_m	S_x	Cultivated mandarin	*C. reticulata*	Wang et al, 2017	SRR3750611
18	WLK	S_m	S_{11}	Cultivated mandarin	*C. reticulata*	Wang et al, 2017	SRR3820551
19	20H	S_m	S_x	Cultivated mandarin	*C. reticulata*	Wang et al, 2017	SRR3747635
20	WHPG	S_m	S_2	Cultivated mandarin	*C. reticulata*	Wang et al, 2018	SRR5796644
21	YJNJ	S_m	S_x	Cultivated mandarin	*C. reticulata*	Wang et al, 2018	SRR5796865
22	YSJ	S_m	S_x	Cultivated mandarin	*C. reticulata*	Wang et al, 2017	SRR3750648
23	NFJ	S_m	S_7	Cultivated mandarin	*C. reticulata*	Wang et al, 2017	SRR5796630
24	JGA	S_m	S_2	Cultivated mandarin	*C. reticulata*	Wang et al, 2018	SRR5796822
25	DFZS	S_m	S_x	Cultivated mandarin	*C. reticulata*	Wang et al, 2018	SRR5807899
26	SM	S_m	S_x	Cultivated mandarin	*C. reticulata*	Wang et al, 2018	SRR5807909
27	WZ	S_m	S_8	Cultivated mandarin	*C. reticulata*	Wang et al, 2018	SRR5807910
28	KYM	S_m	S_7	Cultivated mandarin	*C. reticulata*	Wang et al, 2017	SRR3820643
29	CLP	S_m	S_x	Cultivated mandarin	*C. reticulata*	Wu et al, 2018	SRR6188441
30	CSM	S_m	S_x	Cultivated mandarin	*C. reticulata*	Wu et al, 2018	SRR6188440
31	KSH	S_m	S_7	Cultivated mandarin	*C. reticulata*	Wu et al, 2018	SRR6188456
32	DNC	S_m	S_x	Cultivated mandarin	*C. reticulata*	Wu et al, 2018	SRR6188439
33	KNG	S_m	S_8	Cultivated mandarin	*C. reticulata*	Wu et al, 2018	SRR6188438
34	SNK	S_m	S_x	Cultivated mandarin	*C. reticulata*	Wu et al, 2018	SRR6188455
35	S6	S_m	S_2	Cultivated mandarin	*C. reticulata*	In this study	SRR10163366
36	S8	S_m	S_2	Cultivated mandarin	*C. reticulata*	In this study	SRR10163366
37	MSJ	S_x	S_x	Cultivated mandarin	*C. reticulata*	Wang et al, 2017	SRR3751832
38	STJ	S_x	S_2	Cultivated mandarin	*C. reticulata*	Wang et al, 2017	SRR3756933
39	MLTJ	S_x	S_x	Cultivated mandarin	*C. reticulata*	Wang et al, 2017	SRR3750679
40	ZHJ	S_x	S_x	Cultivated mandarin	*C. reticulata*	Wang et al, 2018	SRR5796927
41	DD	S_m	S_x	Sour orange	*C. aurantium*	Wang et al, 2017	SRR3885049
42	BH	S_m	S_5/S_{13}	Sour orange	*C. aurantium*	In this study	SRR9127844
43	HBLT	S_m	S_x	Sour orange	*C. aurantium*	In this study	SRR9127845

44	HP	S_m	S_x	Sour orange	*C. aurantium*	In this study	SRR9127842
45	JJSC	S_m	S_8	Sour orange	*C. aurantium*	In this study	SRR9127843
46	YDL	S_m	S_x	Sour orange	*C. aurantium*	In this study	SRR9127840
47	XGTC	S_m	S_x	Sour orange	*C. aurantium*	In this study	SRR9127841
48	JJDD	S_m	S_x	Sour orange	*C. aurantium*	In this study	SRR9127838
49	DGTC	S_m	S_x	Sour orange	*C. aurantium*	In this study	SRR9127839
50	XHC	S_m	S_x	Sour orange	*C. aurantium*	In this study	SRR9127848
51	Aur	S_m	S_x	Sour orange	*C. aurantium*	Wang et al, 2017	SRR3885125
52	CBSC	S_m	S_5/S_{13}	Sour orange	*C. aurantium*	Wang et al, 2017	SRR3915646
53	HNSC	S_m	S_5/S_{13}	Sour orange	*C. aurantium*	Wang et al, 2017	SRR3926631
54	SCSC	S_m	S_7	Sour orange	*C. aurantium*	Wang et al, 2017	SRR3926581
55	ZGSC	S_m	S_2	Sour orange	*C. aurantium*	Wang et al, 2017	SRR3916939
56	ANJ	S_m	S_5/S_{13}	Sour orange	*C. aurantium*	In this study	SRR9127847
57	BXI	S_m	S_7	Sour orange	*C. aurantium*	In this study	SRR9127857
58	CHG	S_m	S_x	Sour orange	*C. aurantium*	In this study	SRR9127858
59	DFL	S_m	S_7	Sour orange	*C. aurantium*	In this study	SRR9127855
60	GP	S_m	S_x	Sour orange	*C. aurantium*	In this study	SRR9127856
61	GXSJ	S_m	S_x	Sour orange	*C. aurantium*	In this study	SRR9127853
62	HYDD	S_m	S_7	Sour orange	*C. aurantium*	In this study	SRR9127854
63	HZL	S_m	S_x	Sour orange	*C. aurantium*	In this study	SRR9127851
64	KYC	S_m	S_5/S_{13}	Sour orange	*C. aurantium*	In this study	SRR9127852
65	QLJ	S_m	S_x	Sour orange	*C. aurantium*	In this study	SRR9127849
66	XGCC	S_m	S_x	Sour orange	*C. aurantium*	In this study	SRR9127850
67	YG2	S_m	S_x	Sour orange	*C. aurantium*	In this study	SRR9127846
68	AL	S_m	S_7	Sweet orange	*C. sinensis*	Wang et al, 2017	SRR3883626
69	HML	S_m	S_7	Sweet orange	*C. sinensis*	Wang et al, 2017	SRR3883647
70	XSO	S_m	S_7	Sweet orange	*C. sinensis*	Wang et al, 2017	SRR4237671
71	13X	S_m	S_7	Sweet orange	*C. sinensis*	Wang et al, 2017	SRR3884813
72	29B	S_m	S_7	Sweet orange	*C. sinensis*	Wang et al, 2017	SRR3926732
73	JC	S_m	S_7	Sweet orange	*C. sinensis*	Wang et al, 2017	SRR3884491
74	SO3	S_m	S_x	Sweet orange	*C. sinensis*	Wang et al, 2017	SRR5799051
75	LQ	S_m	S_7	Sweet orange	*C. sinensis*	Wang et al, 2017	SRR3884773
76	NHE	S_m	S_x	Sweet orange	*C. sinensis*	Wang et al, 2017	SRR3927459
77	WSO	S_m	S_7	Sweet orange	*C. sinensis*	Wang et al, 2017	SRR4240447
78	GXY	S_9/S_{12}	S_8	Pummelo	*C. maxima*	Wang et al, 2017	SRR5802549
79	STY	S_1	S_2	Pummelo	*C. maxima*	Wang et al, 2017	SRR5796631
80	WSY	S_4	S_2	Pummelo	*C. maxima*	Wang et al, 2017	SRR5796633
81	10Z	S_3	S_5/S_{13}	Pummelo	*C. maxima*	Wang et al, 2017	SRR3823645
82	GBY	S_3	S_1	Pummelo	*C. maxima*	Wang et al, 2017	SRR3823447
83	HNHY	S_1	S_8	Pummelo	*C. maxima*	Wang et al, 2017	SRR3823230
84	WBY	S_2	S_5/S_{13}	Pummelo	*C. maxima*	Wang et al, 2017	SRR3823251
85	CHP	S_4	S_x	Pummelo	*C. maxima*	Wang et al, 2017	SRR1023627
86	SYBS	S_8	S_2	Pummelo	*C. maxima*	Wang et al, 2017	SRR3844987
87	SYPS	S_1	S_2	Pummelo	*C. maxima*	Wang et al, 2017	SRR3824065
88	MaJia	S_x	S_x	Pummelo	*C. maxima*	Wang et al, 2017	SRR3822290
89	HB	S_7	S_2	Pummelo	*C. maxima*	In this study	SRR9127779
90	SMST	S_1	S_3	Pummelo	*C. maxima*	In this study	SRR9127778

91	YNMD	S_5/S_{13}	S_x	Pummelo	*C. maxima*	In this study	SRR9127777
92	YNSJ	S_6	S_5/S_{13}	Pummelo	*C. maxima*	In this study	SRR9127776
93	ZGST	S_5/S_{13}	S_3	Pummelo	*C. maxima*	In this study	SRR9127780
94	2011-GL-1	S_{10}	S_x	Pummelo	*C. maxima*	Wang et al, 2017	SRR3858312
95	CQ-016	S_{11}	S_x	Pummelo	*C. maxima*	Wang et al, 2017	SRR3822303
96	JA-02	S_5/S_{13}	S_x	Pummelo	*C. maxima*	Wang et al, 2017	SRR3823148
97	Q-04	S_9/S_{12}	S_x	Pummelo	*C. maxima*	Wang et al, 2017	SRR3823455
98	RL-06	S_5/S_{13}	S_x	Pummelo	*C. maxima*	Wang et al, 2017	SRR3823409
99	NJYPS	S_{10}	S_x	Pummelo	*C. maxima*	Wang et al, 2017	SRR3848607
100	AJH	S_8	S_x	Pummelo	*C. maxima*	Wang et al, 2018	SRR5802532
101	HHHXY	S_8	S_x	Pummelo	*C. maxima*	Wang et al, 2018	SRR5802565
102	HHSWY	S_x	S_x	Pummelo	*C. maxima*	Wang et al, 2018	SRR5802582
103	14J	S_m	S_2	Grapefruit	*C. paradisi*	Wang et al, 2017	SRR3926757
104	Ruby	S_m	S_3	Grapefruit	*C. paradisi*	Wang et al, 2017	SRR3927447
105	HJ	S_m	S_x	Grapefruit	*C. paradisi*	In this study	SRR9128709
106	Flame	S_m	S_3	Grapefruit	*C. paradisi*	Wang et al, 2017	SRR3927405
107	PAR	S_m	S_3	Grapefruit	*C. paradisi*	Wu et al, 2018	SRR6188447
108	JY22	S_m	S_2	Lemon	*C. limon*	Wang et al, 2017	SRR3948190
109	YLK	S_m	S_2	Lemon	*C. limon*	Wang et al, 2017	SRR3952134
110	FMN	S_m	S_2	Lemon	*C. limon*	Wang et al, 2017	SRR3951937
111	LS	S_m	S_2	Lemon	*C. limon*	Wang et al, 2017	SRR3948277
112	ALN	S_m	S_2	Lemon	*C. limon*	In this study	SRR9129151
113	FMNL	S_m	S_2	Lemon	*C. limon*	In this study	SRR9129150
114	L-17	S_m	S_2	Lemon	*C. limon*	In this study	SRR9129149
115	N4	S_m	S_2	Lemon	*C. limon*	In this study	SRR9129148
116	POST	S_m	S_2	Lemon	*C. limon*	In this study	SRR9129154
117	YN	S_m	S_2	Lemon	*C. limon*	In this study	SRR9129153
118	WLF	S_m	S_2	Lemon	*C. limon*	Wang et al, 2017	SRR3952242
119	05L-06	S_m	S_2	Lemon	*C. limon*	In this study	SRR9129152
120	JY	S_9/S_{12}	S_x	Citron	*C. medica*	Wang et al, 2017	SRR3938734
121	XZ1	S_x	S_x	Citron	*C. medica*	Wang et al, 2017	SRR3938253
122	JY15	S_1	S_x	Citron	*C. medica*	Wang et al, 2017	SRR3944177
123	JY28	S_9/S_{12}	S_x	Citron	*C. medica*	Wang et al, 2017	SRR3948093
124	JY4	S_3	S_x	Citron	*C. medica*	Wang et al, 2017	SRR3944125
125	JY5	S_9/S_{12}	S_x	Citron	*C. medica*	Wang et al, 2017	SRR3944139
126	JY8	S_5/S_{13}	S_x	Citron	*C. medica*	Wang et al, 2017	SRR3944160
127	XZ	S_{14}	S_x	Citron	*C. medica*	Wang et al, 2017	SRR3938056
128	DYC	S_x	S_x	Ichang papeda	*C. ichangensis*	Wang et al, 2017	SRR3929735
129	JF	S_x	S_x	Ichang papeda	*C. ichangensis*	Wang et al, 2017	SRR3929760
130	KM	S_9/S_{12}	S_x	Ichang papeda	*C. ichangensis*	Wang et al, 2017	SRR3929763
131	PY11	S_x	S_x	Ichang papeda	*C. ichangensis*	Wang et al, 2017	SRR3928244
132	TK	S_x	S_x	Ichang papeda	*C. ichangensis*	Wang et al, 2017	SRR3929810
133	XJC	S_5/S_{13}	S_x	Ichang papeda	*C. ichangensis*	Wang et al, 2017	SRR3928212
134	YCC	S_x	S_{11}	Ichang papeda	*C. ichangensis*	Wang et al, 2017	SRR3928564
135	YCLS	S_x	S_x	Ichang papeda	*C. ichangensis*	Wang et al, 2017	SRR3929790
136	YCYJ	S_x	S_x	Ichang papeda	*C. ichangensis*	Wang et al, 2017	SRR3929943
137	YL	S_5/S_{13}	S_{10}	Ichang papeda	*C. ichangensis*	Wang et al, 2017	SRR3930078

138	ZY	S_x	S_x	Ichang papeda	*C. ichangensis*	Wang et al, 2017	SRR3931949
139	Ace	S_x	S_x	Atalantia	*A. buxifolia*	Wang et al, 2017	SRR3988226
140	Amo	S_x	S_x	Atalantia	*A. buxifolia*	Wang et al, 2017	SRR3989253
141	ARO	S_9/S_{12}	S_1	Atalantia	*A. buxifolia*	Wang et al, 2017	SRR3989264
142	CDSJ	S_x	S_1	Atalantia	*A. buxifolia*	Wang et al, 2017	SRR3989910
143	GDMM	S_x	S_x	Atalantia	*A. buxifolia*	Wang et al, 2017	SRR3990142
144	HDGKZ	S_x	S_x	Atalantia	*A. buxifolia*	Wang et al, 2017	SRR3990145
145	HKC	S_9/S_{12}	S_2	Atalantia	*A. buxifolia*	Wang et al, 2017	SRR3988729
146	JBL	S_x	S_x	Atalantia	*A. buxifolia*	Wang et al, 2017	SRR3988460
147	JMPG1	S_1	S_6	Atalantia	*A. buxifolia*	Wang et al, 2017	SRR3990571
148	JMPG2	S_x	S_x	Atalantia	*A. buxifolia*	Wang et al, 2017	SRR3990663
149	Sdi	S_x	S_x	Atalantia	*A. buxifolia*	Wang et al, 2017	SRR3989214
150	SND	S_1	S_5/S_{13}	Atalantia	*A. buxifolia*	Wang et al, 2017	SRR3990714
151	WNNL	S_x	S_5/S_{13}	Atalantia	*A. buxifolia*	Wang et al, 2017	SRR3990759
152	WNSMW	S_6	S_x	Atalantia	*A. buxifolia*	Wang et al, 2017	SRR3992564
153	WSD	S_x	S_x	Atalantia	*A. buxifolia*	Wang et al, 2017	SRR3992888

Genome sequences of 153 citrus accessions containing published and unpublished sources were mapped to 15 *S-RNase* sequences. As a result, 132/153 accessions were found to contain these *S-RNase* genes and 90/153 accessions harbor the S_m*-RNase* gene.

[a]: We assumed all accessions were heterozygous with two *S*-haplotypes segregating. S_x*-RNase* indicates the unmapped *S*-haplotypes.

Note that the sequences between S_9*-RNase* and S_{12}*-RNase* and between S_5*-RNase* and S_{13}*-RNase* are so highly similar that these pairs of genes cannot be distinguished from each other through reads mapping.

References for Supplemental Information

1 Kheyr-Pour, A. *et al.* Sexual plant reproduction sequence diversity of pistil S-proteins associated with gametophytic selfincompatibility in *Nicotiana alata*. *Sex. Plant Reprod.* **3**, 88-97 (1990).

2 Eddy, S. R. A new generation of homology search tools based on probabilistic inference. *Genome Inform.* **23**, 205-211 (2009).

3 Liang, M. *et al.* Genome-wide identification and functional analysis of S-RNase involved in the self-incompatibility of citrus. *Mol. Genet. Genomics* **292**, 325-341 (2017).

4 Nowak, M. D., Davis, A. P., Anthony, F. & Yoder, A. D. Expression and trans-specific polymorphism of self-incompatibility RNases in *coffea* (Rubiaceae). *PloS One* **6**, e21019 (2011).

5 Asquini, E. *et al.* S-RNase-like sequences in styles of *Coffea* (Rubiaceae). Evidence for S-RNase based gametophytic self-Incompatibility? *Trop. Plant Biol.* **4**, 237-249 (2011).

6 Ramanauskas, K. & Igić, B. The evolutionary history of plant T2/S-type ribonucleases. *PeerJ* **5**, e3790 (2017).

7 Tsuchimatsu, T. *et al.* Patterns of polymorphism at the self-incompatibility locus in 1,083 *Arabidopsis thaliana* genomes. *Mol. Biol. Evol.* **34**, 1878-1889 (2017).

8 Kubo, K. *et al.* Collaborative non-self recognition system in S-RNase–based self-incompatibility. *Science* **330**, 796-799 (2010).

9 Kubo, K. *et al.* Gene duplication and genetic exchange drive the evolution of S-RNase-based self-incompatibility in *Petunia*. *Nat. Plants* **1**, 14005 (2015).

10 Workenhe, S. T., Kibenge, M. J. T., Iwamoto, T. & Kibenge, F. S. B. Absolute quantitation of infectious salmon anaemia virus using different real-time reverse transcription PCR chemistries. *J. Virol. Methods* **154**, 128-134 (2008).

11 Ida, K. *et al.* The 1.55 Å resolution structure of *Nicotiana alata* S_{F11}-RNase associated with gametophytic self-incompatibility. *J. Mol. Biol.* **314**, 103-112 (2001).

12 Wang, X. *et al.* Genomic analyses of primitive, wild and cultivated citrus provide insights into asexual reproduction. *Nat. Genet.* **49**, 765-772 (2017).

13 Xue, Y., Carpenter, R., Dickinson, H. G. & Coen, E. S. Origin of allelic diversity in antirrhinum *S* locus RNases. *Plant Cell* **8**, 805-814 (1996).

14 Ushijima, K. *et al.* Cloning and characterization of cDNAs encoding S-RNases from almond (*Prunus dulcis*): primary structural features and sequence diversity of the S-RNases in Rosaceae. *Mol. Gen. Genet.* **260**, 261-268 (1998).

15 Mir, J. *et al.* Molecular identification of S-alleles associated with self-incompatibility in apple (Malus spp.) genotypes. *Indian J. Agr. Sci.* **86**, 78-81 (2016).

16 Fujii, S., Kubo, K.-i. & Takayama, S. Non-self- and self-recognition models in plant self-incompatibility. *Nat. Plants* **2**, 16130 (2016).

17 Wang, L. *et al.* Genome of wild mandarin and domestication history of mandarin. *Mol. Plant* **11**, 1024-1037 (2018).

18 Wu, G. A. *et al.* Genomics of the origin and evolution of *Citrus*. *Nature* **554**, 311-316 (2018).